

Geology, Mineralization, Fluid Inclusion and Stable Isotope of the Early Cretaceous Sn and Associated Metal Deposits in the Southern Great Xing'an Range, NE China: A Review



WANG Chengyang^{1,*}, LIU Guanghu¹, SUN Zhenjun¹, LIU Jie¹, LI Jianfeng² and LIANG Xinyang¹

¹ Institute of Disaster Prevention, Sanhe, Hebei 065201, China

² College of Urban and Environmental Science, Liaoning Normal University, Dalian, Liaoning 116029, China

Abstract: The Southern Great Xing'an Range (SGXR) hosts a number of Early Cretaceous Sn and associated metal deposits, which can be divided into three principal types according to their geological characteristics: skarn type deposits, porphyry type deposits and hydrothermal vein type deposits. Fluid inclusion assemblages of different types of deposits are quite different, which represent the complexities of metallogenic process and formation mechanism. CH₄ and CO₂ have been detected in fluid inclusions from some of deposits, indicating that the ore-forming fluids are affected by materials of Permian strata. Hydrogen and oxygen isotope data from ore minerals and associated gangue minerals indicate that the initial ore fluids were dominated by magmatic waters, some of which had clearly exchanged oxygen with wall rocks during their passage through the strata. The narrow range for the δ³⁴S values presumably reflects the corresponding uniformity of the ore-forming fluids, and these δ³⁴S values have been interpreted to reflect magmatic sources for the sulfur. The comparison between lead isotope ratios of ore minerals and different geological units' also reveals that deeply seated magma has been a significant source of lead in the ores.

Key words: fluid inclusion, stable isotope, Early Cretaceous Sn and associated metal deposits, Southern Great Xing'an Range

Citation: Wang et al., 2019. Geology, Mineralization, Fluid Inclusion and Stable Isotope of the Early Cretaceous Sn and Associated Metal Deposits in the Southern Great Xing'an Range, NE China: A Review. Acta Geologica Sinica (English Edition), 93(5): –. DOI: 10.1111/1755-6724.14390

1 Introduction

The Southern Great Xing'an Range (SGXR) is one of the most important non-ferrous metal ore concentrating areas in northeastern China, and this district has been listed as one of 19 key belts that are often targets for mineral exploration in China (Wu et al., 2008). Ore deposits of different types and sizes have been found and mined over the past decades in this area. Besides the newly discovered deposits, the number of mineral resources from known deposits has also increased in recent years, making this belt a continuous hot area for ore deposit research in northern China (Liu et al., 2004; Zeng et al., 2011; Mei et al., 2015;). Fig. 1c shows the location of many of the major deposits in SGXR.

During the past years, geologists have carried out a lot of work on geochronology to accurately constrain the ages of these deposits (Zhou et al., 2010a, b; Zhou et al., 2012; Wan et al., 2014; Li et al., 2016; Liu et al., 2016; Liu et al., 2018). And the results reveal that polymetallic mineralization in SGXR was mainly occurred in Early-Middle Permian, Early-Middle Triassic, Early Jurassic and Early Cretaceous (Ouyang et al., 2015). Ore deposits of Early Cretaceous constitute the most important part of

hydrothermal mineralization in SGXR. The major Early Cretaceous Sn and associated metal deposits from SGXR can be divided into three types on the basis of their mineral assemblages, host rocks and major ore controlling factors: (1) skarn type deposits, (2) porphyry type deposits, and (3) hydrothermal vein type deposits (Wang, 2015; Table 1). Since 2010s, we have successively carried out study on geology, fluid inclusion, stable isotope, litho-geochemistry, geochronology and metallogenic prediction of Haobugao, Huanggang, Dongshanwan, Shuangjianzishan, Bairendaba, Bujinhei and Dajing deposit in the area, and the corresponding achievements have been published in periodicals of China or abroad (Wan et al., 2014; Li et al., 2016; Zhang et al., 2017; Wang et al., 2018a, b; Wang et al., 2019).

This paper will review the geology, fluid inclusion and isotope of the Early Cretaceous hydrothermal Sn and associated metal deposits, which is based on the data compiled from the authors' own work and other articles. And the temporal, spatial and genetic relationships between different types of ore deposits are also discussed in this paper. All of the deposits presented in this paper have high-precision ages of mineralization which are defined by radio isotopic dating methods.

* Corresponding author. E-mail: 598648597@qq.com

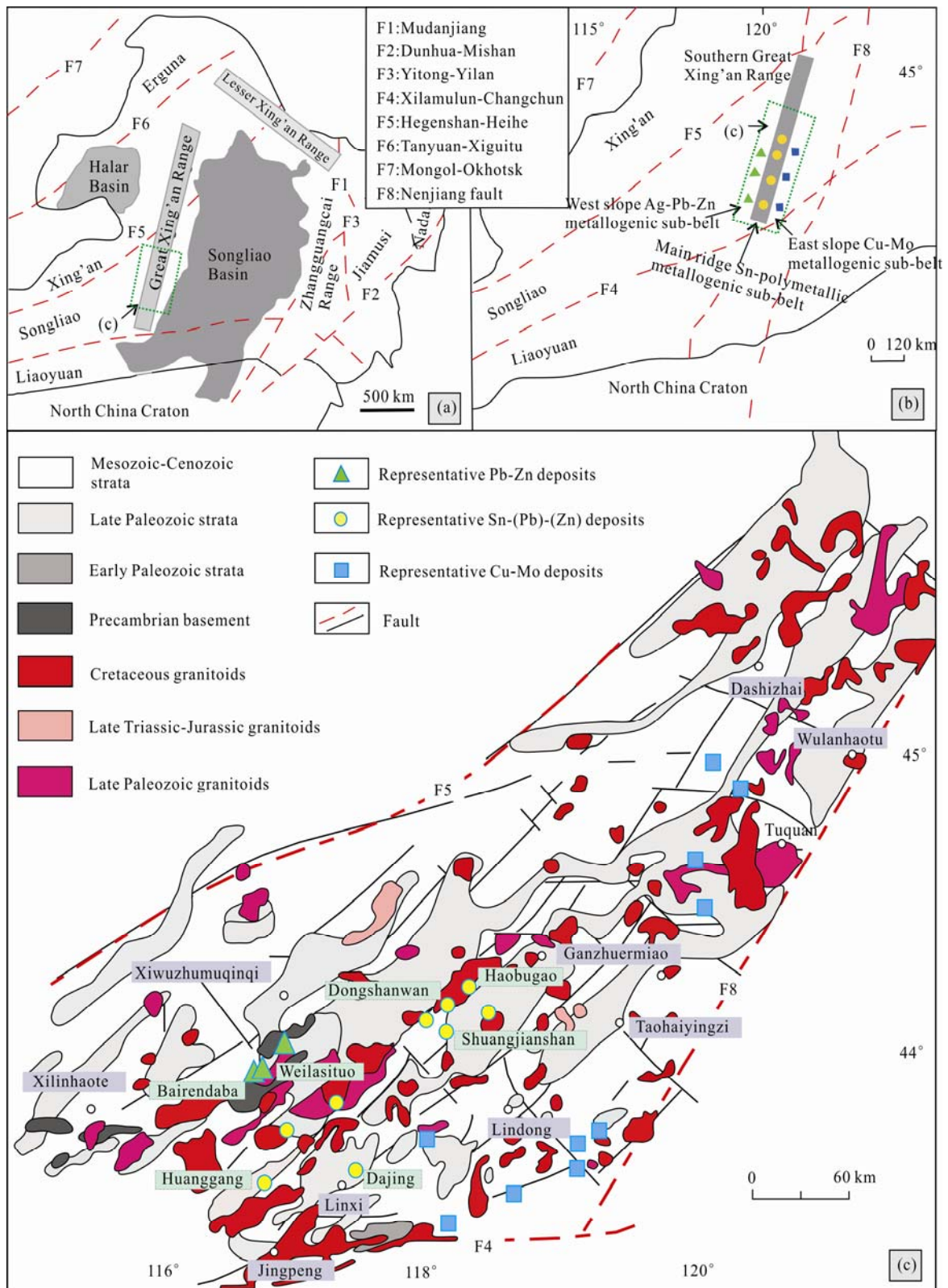


Fig. 1. (a) Tectonic subdivisions of NE China; (b) tectonic subdivisions of the Great Xing'an Range; (c) regional geological map of the southern Great Xing'an Range. a is after Wu et al. (2011), b is after Liu et al. (2004) and c is after Zeng et al. (2011).

Table 1 Geological features of Early Cretaceous deposits from Southern Great Xing'an Range

Ore deposit type	Ore deposit name	Metallogenic elements	Types of intrusion	Surrounding rock strata	Age of intrusion/ analysis method	Age of mineralization analysis method	Reference
Skarn type	Haobugao	Cu-Pb-Zn-Ag-Fe-Sn	Alkali feldspar granite, granite porphyry, fine grained granite	Marble, silty slate, andesite of Permian Dashizhai Formation	136.7–144.8 Ma/ LA-ICP-MS Zircon U-Pb	140.3Ma/Molybdenite Re-Os; 142.9±1.6 Ma/Cassiterite U-Pb	Our previous study; Liu, et al., 2018
	Huanggang	Fe-Sn-W-(Pb)- (Zn)	Alkali feldspar granite Granite porphyry	Marble and andesite of Huanggangliang Formation	136.7–136.8 Ma/ LA-ICP-MS Zircon U-Pb	135.31±0.85 Ma/Molybdenite Re-Os	Zhou et al., 2010;
Porphyry type	Dongshanwan	W-Mo-Sn-Cu-Pb-Zn	Granite porphyry	Silty slate of Permian Dashizhai Formation	142.2±0.9 Ma/ LA-ICP-MS Zircon U-Pb	140.4±1.8 Ma/ Molybdenite Re-Os	Our previous study
	North Haobugao	Cu-Mo-(Pb)- (Zn)	Granite porphyry, porphyritic granite	/	142.2±0.9 Ma/ LA-ICP-MS Zircon U-Pb	139–141 Ma/ Molybdenite Re-Os	Our previous study
Hydrothermal vein type	Dajing	Sn-Cu-Pb-Zn-Ag	andesitic porphyry, quartz porphyry	Siltstone, fine sandstone, marl, shale of Permian Linxi formation	133.2Ma and 146.1Ma/ LA-ICP-MS Zircon U-Pb	140 Ma/ Sericite Ar-Ar	Chu et al., 2002; Niu et al., 2006; Feng et al., 1994; Jiang et al., 2010
	Bairendaba	Pb-Zn-Ag-(Cu)	Quartz diorite, granic vein	Biotite plagiogneiss and of Baoyintu Group; Hercynian quartz diorite	326.5 and 318 Ma/ LA-ICP-MS Zircon U-Pb;	135 Ma/ Muscovite ⁴⁰ Ar- ³⁹ Ar;	Ouyang, 2013; Liu et al, 2014; Chang et al, 2010
	Weilasituo	Sn-Cu-Zn-(Ag)	quartz porphyry	Biotite plagiogneiss and of Baoyintu Group; Hercynian quartz diorite	135 Ma / LA-ICP-MS Zircon U-Pb	133 Ma/Muscovite ⁴⁰ Ar- ³⁹ Ar; 135 Ma / Molybdenite Re-Os; 135–138 Ma/ Cassiterite U-Pb	Pan et al., 2009; Zhai et al., 2016; Liu et al., 2016; Wang et al., 2017

2 Geological Setting

As one of the most important economic mineral districts in northern China, the SGXR is tectonically located in the eastern part of the Xingmeng orogenic belt (Xiao et al., 2013). The Xilinhot Complex, which was proposed to be formed in the Mesoproterozoic, is the oldest stratigraphic unit exposed in the area. The previous studies have indicated that the Xilinhot Complex mainly consists of deformed and metamorphosed rocks. And the main rock types include biotite-(garnet)-plagioclase gneiss, biotiteplagioclase gneiss, sillimanite-biotite-plagioclase gneiss, biotite-(hornblende)-plagioclase migmatite, amphibolites and gneissic granite. Regionally, the Xilinhot Complex is intruded by Late Proterozoic basic-ultrabasic rocks and Phanerozoic granites (Ge et al., 2011; Wu et al., 2011; Zhou and Ge, 2013). The Xilinhot Complex is also one of the most significant ore-bearing stratigraphic units in the study area, and the famous Bairendaba and Weilasituo deposits occur in it. Except for the Xilinhot Complex, the strata exposed in the regional area are mainly composed of Late Paleozoic and Mesozoic Formations. The Carboniferous strata in the regional area mainly consist of the Benbatu and Amushan formation. The Benabtu Formation is composed of sandstone, feldspar sandstone and conglomerate, and the Amushan formation consists of two transitional lithofacies, varying from marine clastics to carbonates (Bao et al., 2006). The Permian strata, mainly including the Dashshzhai, Huanggangliang and Linxi Formation, is the most important ore bearing strata in SGXR. The lithologies of Permian strata mainly consist of altered volcanic rocks, spillite-keratophyre, metasandstone, slate and marble (Li et al., 2010). Mesozoic strata in the regional area include the Lower Jurassic Hongqi Formation, the Upper Jurassic Manketouebo formation and the Lower Cretaceous

Manitu, Baiyingaolao and Meiletu Formation. The Lower Jurassic Hongqi Formation is mainly composed of conglomerate, sandstone, siltstone, mudstone and coal. The Upper Jurassic-Lower Cretaceous strata mainly contain continental volcanic rocks, which are composed of basaltic andesite, rhyolite and felsic volcanic tuff (Ying et al., 2011).

The structures in SGXR are mainly distributed in NE-trending, near EW- trending, NWW- and NW- trending. The EW- trending structures formed in an earlier tectonic system, which is related to the closure of the Paleo-Asian Ocean. The NE- trending structure is the major structure of SGXR, which controls the distribution of the majorities of intrusions and ore deposits. The NWW and NW trending faults constitute the derivative structures in the regional area (Zhao and Zhang, 1997; Sheng and Fu, 1999).

The previous study has divided the SGXR into the following four important mineralization concentration zones: the Xilinhot–Huolinguole Ag–polymetallic zone, Linxi–Ganzhuermiao Sn–Cu–polymetallic zone, Tianshan Mo–polymetallic zone, and Tuquan Cu–polymetallic zone (Ouyang et al., 2015). Most of the ore deposits in SGXR are hosted in Permian rocks and are temporally, spatially, genetically associated with Mesozoic intrusions (Liu et al., 2004; Niu et al., 2009; Shao et al., 2010).

3 General Descriptions of Ore Deposits

3.1 Skarn type deposit

Three important skarn type deposits occur in SGXR, namely, Huanggang, Haobugao and Baiyinnuoer. Our previous research of molybdenite Re–Os dating shows that the Haobugao deposit is formed at 140.3 Ma, and the mineralization related granites in the mining area are formed between 136.7–144.8 Ma based on the LA-ICP-

MS U-Pb dating of the zircons (Wan et al., 2014; Liet et al., 2015; Wang, 2015). Besides, Liu et al. (2018) obtained similar mineralization age of 139 ± 0.6 Ma through cassiterite LA-ICP-MS U-Pb dating method. Researches of Zhou et al. (2010a) show that the Huanggang deposit is formed at 135.8 Ma (molybdenite Re–Os dating), and the mineralization related granite in the deposit is formed at 136.6–136.8 Ma (LA-ICP-MS zircon U-Pb dating; Zhou et al., 2010b). As mentioned above, the existing researches clearly show that Haobugao and Huanggang deposits are both belong to skarn type deposits which are genetically related to Early Cretaceous magmatism. While the formation age of Baiyinnuoer deposit is still controversial between scholars till the present moment: (1) Jiang et al. (2011) believes that the deposit is genetically related to Triassic diorite, and the metallogenic age is determined to be 244.5 Ma through a zircon U-Pb method. (2) The results of Rb-Sr dating show that sphalerites from the deposit are formed at 167.6 Ma (Wang, 2017), and the age is consistent with the ages of tuff lava exposed in the mining area. (3) Quartz porphyry vein with zircon U-Pb age of 129 Ma, is the only Cretaceous intrusion which is ever found in the mining area (Jiang et al., 2011). However, the vein obviously cuts through skarns and oredodies, indicating that it should be the product of the magmatism after Pb-Zn mineralization.

3.1.1 Haobugao deposit

The Haobugao deposit is a large size skarn-type deposit which is located in SGXR. Besides the Quaternary, the stratigraphic units exposed in the mining area mainly consist of the Upper Jurassic Manketouebo Formation and the Lower Permian Dashizhai Formation (Fig. 2a). The Dashizhai Formation, which is the major ore-hosting strata of this area, mainly consists of marine pyroclastic rocks, slate, argillaceous siltstone, and marble. The Jurassic Manketouebo Formation, which is composed of rhyolitic pyroclastic rocks, and unconformably overlies the Permian strata (Liu et al., 2017; Wang et al., 2018).

The main structures in the ore district contain the NE-trending Haobugao anticline, and the NE-, NNW-, NW-trending faults. The Haobugao anticline is an overturned anticline with the axial direction of NE-SW. The NE-trending faults, combined with the NE-trending anticline, constitute the major ore-controlling structures in the mining area. The NNW- and NW-trending faults cut across the pre-existing NE-trending structures, indicating that they are formed later than mineralization. Intrusive rocks in the ore district mainly include the Wulanba Granite and Wulanchulute Granite, our published geochronological and geochemical data show that both of the intrusions are belonged to Early Cretaceous A-type granites (Li et al., 2015).

The deposit is positioned along the contact between Early Cretaceous intrusions and Permian carbonate rocks (Fig. 2b). Until now, the industrial ore bodies in this area are mainly located in the south-eastern flank of the rollover anticline, and the prospecting potential of the north-western flank of Haobugao anticline can not to be neglected. Ore textures provide direct clues for tracking ore-forming processes, according to the

occurrence of mineral assemblages and the ore textures, the paragenetic sequence during formation of Haobugao deposit can be divided into four mineralizing stages: skarn stage, iron-tin oxide stage, early quartz sulfide stage and late quartz-sulfide stage. The skarn stage is the earliest paragenetic stage which is dominated by prograde skarn minerals, including pyroxene, garnet and wollastonite (Fig. 3). The oxide stage comprises abundant magnetite, retrograde hydrous skarn minerals and minor cassiterite. The magnetites and retrograde hydrous skarn minerals, such as amphibole and chlorite of this stage either replace or occur with earlier skarn minerals. The early quartz-sulfide stage consists of arsenopyrite, pyrite, chalcopyrite, sphalerite, pyrrhotite and bornite, and the gangue minerals of this stage include quartz, chlorite and minor fluorite. The late quartz-sulfide stage is characterized by sphalerite, galena and abundant calcite and quartz.

3.1.2 Huanggang deposit

The Huanggang deposit is the largest tin-based multi-metal deposit in the northern part of the North China Plate (Zhou et al., 2010a). Four Permian stratigraphic units, including the Lower Permian Qingfengshan Formation, Dashizhai Formation, Huanggangliang Formation, and the Upper Permian Linxi Formation, exposed in the Huanggangliang area (Fig. 4). The Sn-Fe mineralization developed along the contact zone between Early Cretaceous granites and Permian strata, and mineralization of the deposit is spatially and temporally linked to the skarn. It is generally accepted that the majority of skarns and skarn type deposits are found in lithologies containing at least some carbonate rocks, such as limestone and marble, but in Huanggang deposit, a important geological phenomenon is that parts of the ore bodies occur in the outer contact zone between intrusive rocks and Permian andesites.

Intrusive rocks in the Huanggang area are mainly composed of K-feldspar-bearing granites and granite porphyries. The geochemical and geochronological research indicated that the Huanggangliang intrusion belongs to Early Cretaceous A-type granites which related to lithospheric thinning (Zhou et al., 2010b). Magnetite, hematite, cassiterite, varlamoffite, sphalerite, scheelite, loellingite, chalcopyrite constitute the main ore minerals of the ores, which display a variety of textures. Gangue minerals of the deposit were dominated by skarn minerals such as garnet, pyroxene, amphibole, with minor fluorite, calcite, quartz, epidote, chlorite and phlogopite.

The typical textures of ores include subhedral, granular, metasomatic and exsolution textures. The ores of the deposit show mainly massive, breccia, veinlike structures, and minor banded and disseminated structures. The ore-forming process of the deposit can be divided into the four following stages based on field observations, petrographic and mineragraphic observations, and across-cutting and replacement relationships: (1) prograde skarn stage. Mineral assemblage of this stage is mainly composed by pyroxene, garnet, wollastonite and vesuvianite; (2) retrograde alteration stage. This stage is characterized by occurrence of hydrous skarn mineral (hornblende, actinolite, epidote, chlorite and mica); (3) quartz-sulfide

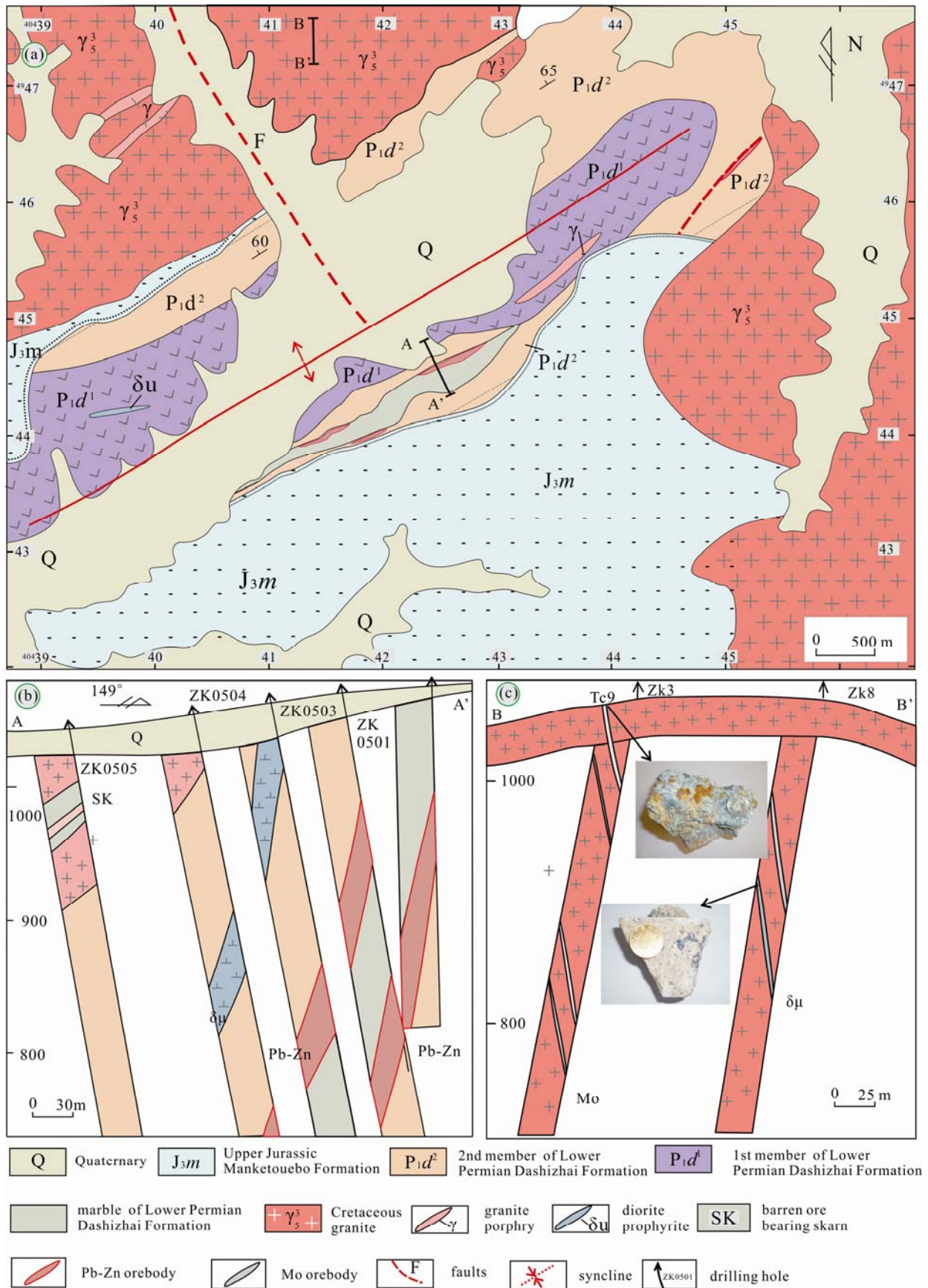


Fig. 2. (a) Geologic map of the Haobugao ore district; (b) cross-section of the Haobugao ore deposit; (c) cross-section of the porphyry type mineralization areas at the periphery of the Haobugao deposit

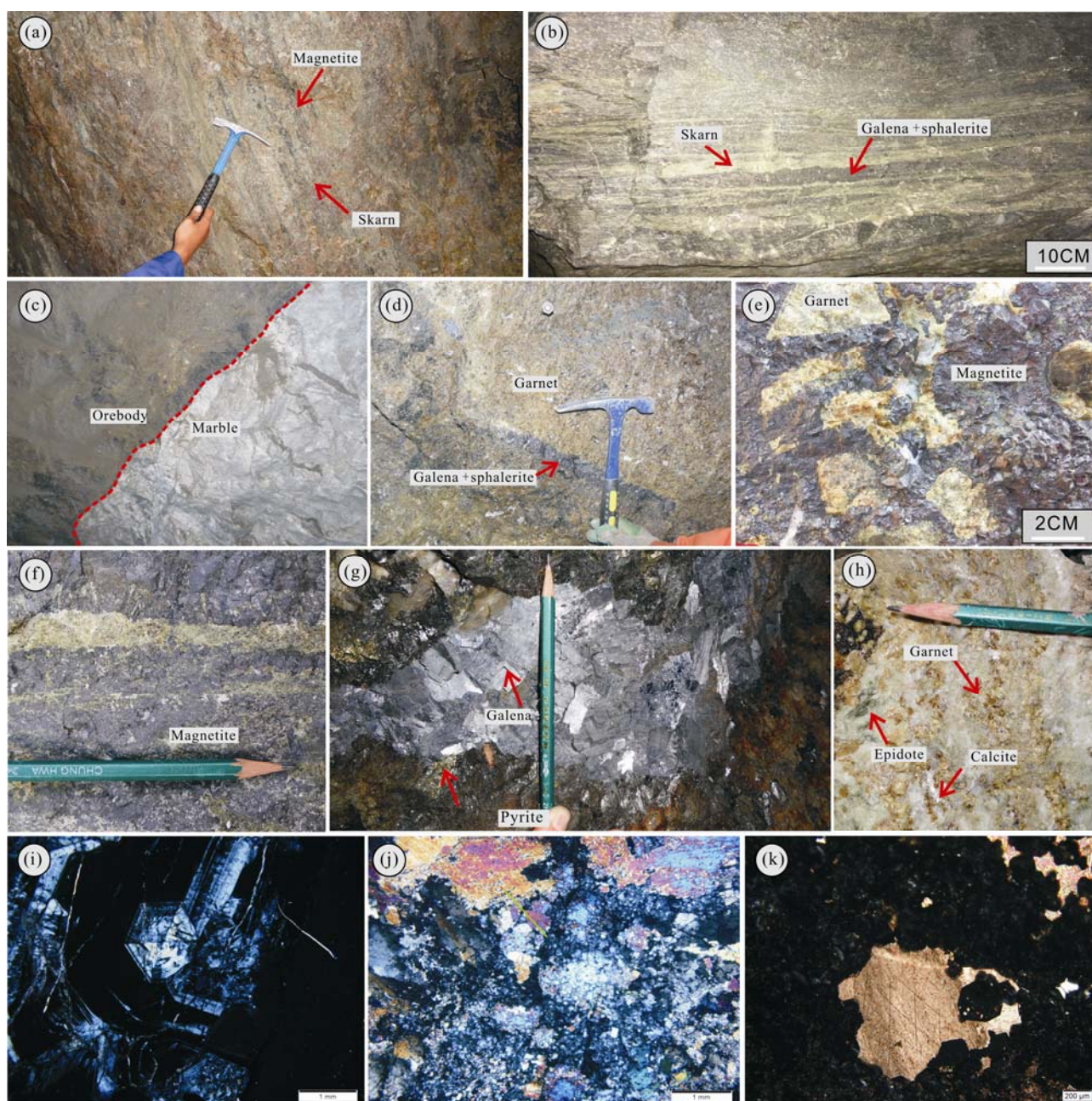


Fig. 3. Macro-, hand-specimen and microscopic scale characteristic for the skarn type deposits from the SGXR.

(a) Rhythmic banded magnetite in skarns, Huanggang; (b) rhythmic banded sulfide ores in skarns, Haobugao; (c) Morphological characteristics of the reaction front from the marble-skarn contact; (d) a sulfide vein occurred in garnet skarn, Haobugao. (e) breccia textures showing breccia fragments cemented by magnetites, Haobugao; (f) euhedral garnet (brown) surrounded by calcite and epidote, Haobugao; (g) euhedral and coarse galena occurred in geode, Huanggang; (h) euhedral garnet particles surrounded by calcite of late mineralization stage; (i) oscillatory zoned garnet, Haobugao; (j) altered tremolite aggregate, Haobugao; (k) calcite occurred in the gap of other minerals, Haobugao.

stage, and metallic mineral assemblage of this stage is dominated by pyrite, chalcopryrite, galena, molybdenite, sphalerite, scheelite and pyrrhotite; (4) carbonate stage. Wall rock alteration styles in the hydrothermal stage are complex, and include skarnization, pyritization, silicification, albitization, chloritization, epidotization, sericitization. Skarnization at Huanggang has formed garnet, pyroxene, diopside, cassiterite and magnetite with associated Fe–Sn mineralization (Fig. 3).

3.2 Porphyry type deposits

Several porphyry type deposit have been found in southern Great Xing'an Range, and most of the deposits are Mo (Cu)-dominated deposits, only a few porphyry type Sn and associated metal deposits have been discovered to date. Dongshanwan is a newly discovered porphyry type W-Mo-Sn-Pb-Zn deposit in recent years, our molybdenite Re-Os and zircon U-Pb dating reveals that the mineralization of Dongshanwan was formed at

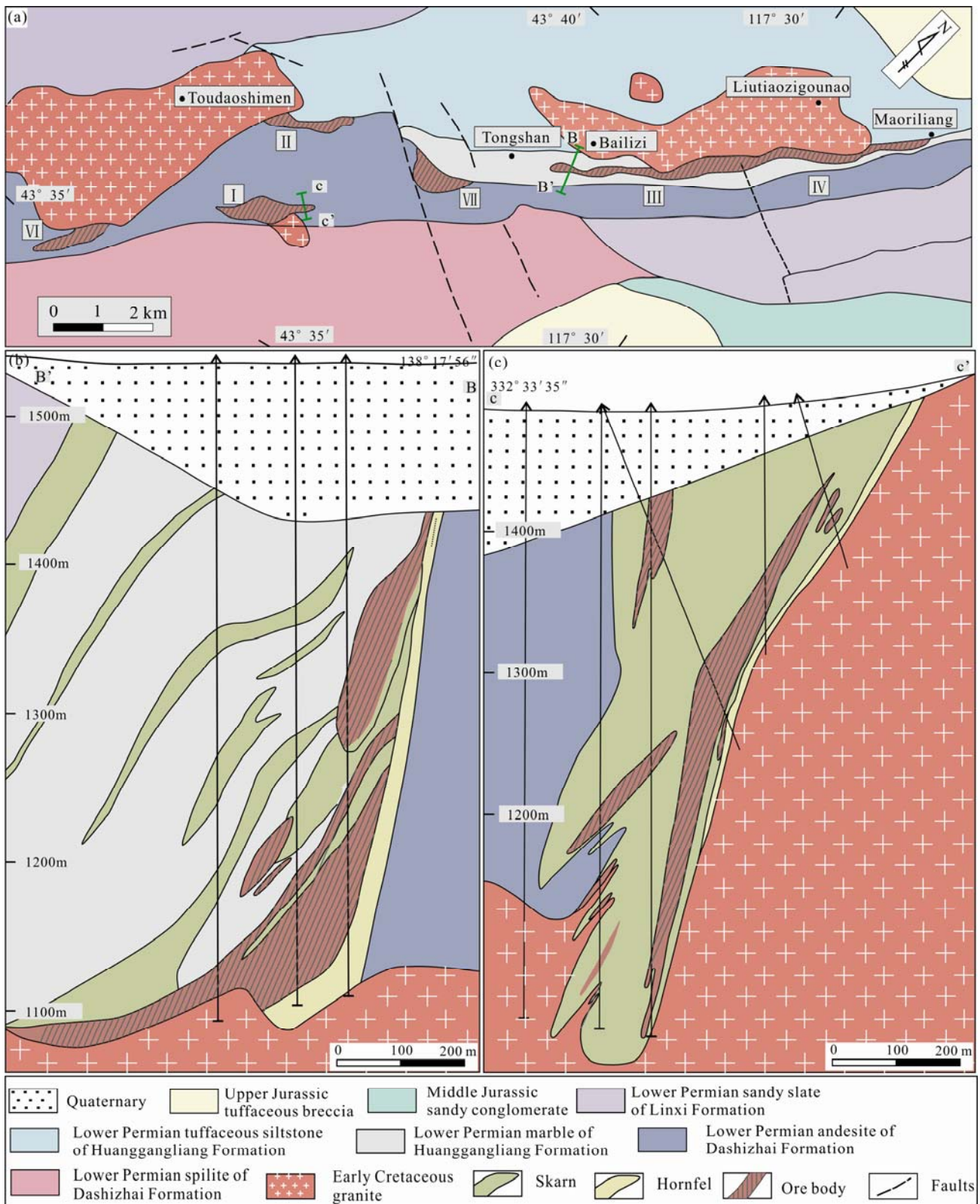


Fig. 4. (a) Geological map of the Huanggang area; (b) geological section along exploration line 70 of SKI district in Huanggang deposit; (c) geological section along exploration line 418 of SKIII district in Huanggang deposit. (modified from Mei, 2015; Zhou et al., 2012)

140.5 Ma, and ore-bearing granite of the deposit was formed at 142.2 Ma. The porphyry-type mineralization

age is consistent with the crystallizing age of ore-bearing granite (Wang, 2015).

Recently, porphyry type Cu-Mo-(Pb)-(Zn) mineralization has also been discovered in the periphery of the mining district of Haobugao deposit, which also indicates that a great potential for discovering porphyry type deposits exist in this area. Our LA-ICP-MS zircon U-Pb dating of granite porphyry yielded a weighted mean $^{206}\text{Pb}/^{238}\text{U}$ age of 141.9 ± 1.2 Ma, which was interpreted as the emplacement age of the granite porphyry, while the model ages of molybdenite Re-Os dating range from 139.9 ± 2.3 Ma to 141.0 ± 1.7 Ma. The molybdenite Re-Os age is quite consistent with the LA-ICP-MS zircon U-Pb age of the host granite, suggesting a coeval and causative relation between the granite and mineralization.

3.2.1 Dongshanwan deposit

Dongshanwan deposit, which was discovered by Team No. 243 of the China National Nuclear Corporation in 2008, is a typical porphyry type deposit with intense mineralization of W, Sn, Mo and Pb, Zn, Ag (Zeng et al., 2015). Dongshanwan deposit is characterized by veinlet-disseminated type mineralization that developed in the Early Cretaceous granite porphyry. According to the location of industrial ore bodies, the ore district can be divided into two ore blocks (Fig. 5). The Block I is

located in the middle part of the mining area, most of the tungsten, molybdenum, silver and polymetallic ores are produced in this block. Up to now, 49 silver polymetallic symbiotic ore bodies, 42 tungsten ore bodies, 32 molybdenum ore bodies, 17 tin orebodies, 9 tungsten-molybdenum orebodies, 2 silver-tungsten orebodies and 2 silver-molybdenum orebodies have been found in this block. The Block II is located in the northern part of the mining area, and only one industrial lead-zinc polymetallic ore body is found in this block. The ore minerals of this deposit are mainly composed of wolframite, cassiterite, molybdenite, arsenopyrite, argyrite, chalcopyrite, galena, malachite, chessylite, etc. The common gangue minerals are K-feldspar, albite, fluorite quartz and sericite. Hydrothermal alteration surrounding the Dongshanwan deposits is generally characterized by concentric zones that range from an inner potassic zone outward to kaolinization-albitization-sericitization-silicification zone, and an outer propylitic zone. The major alteration related to the tungsten-molybdenum mineralization is potassium alteration, silicification and sericitification, while the silver, lead and zinc mineralization is spatially related to propylitization. Similar to the zoning of alteration, strong zoning patterns in metals and ore mineralogy also

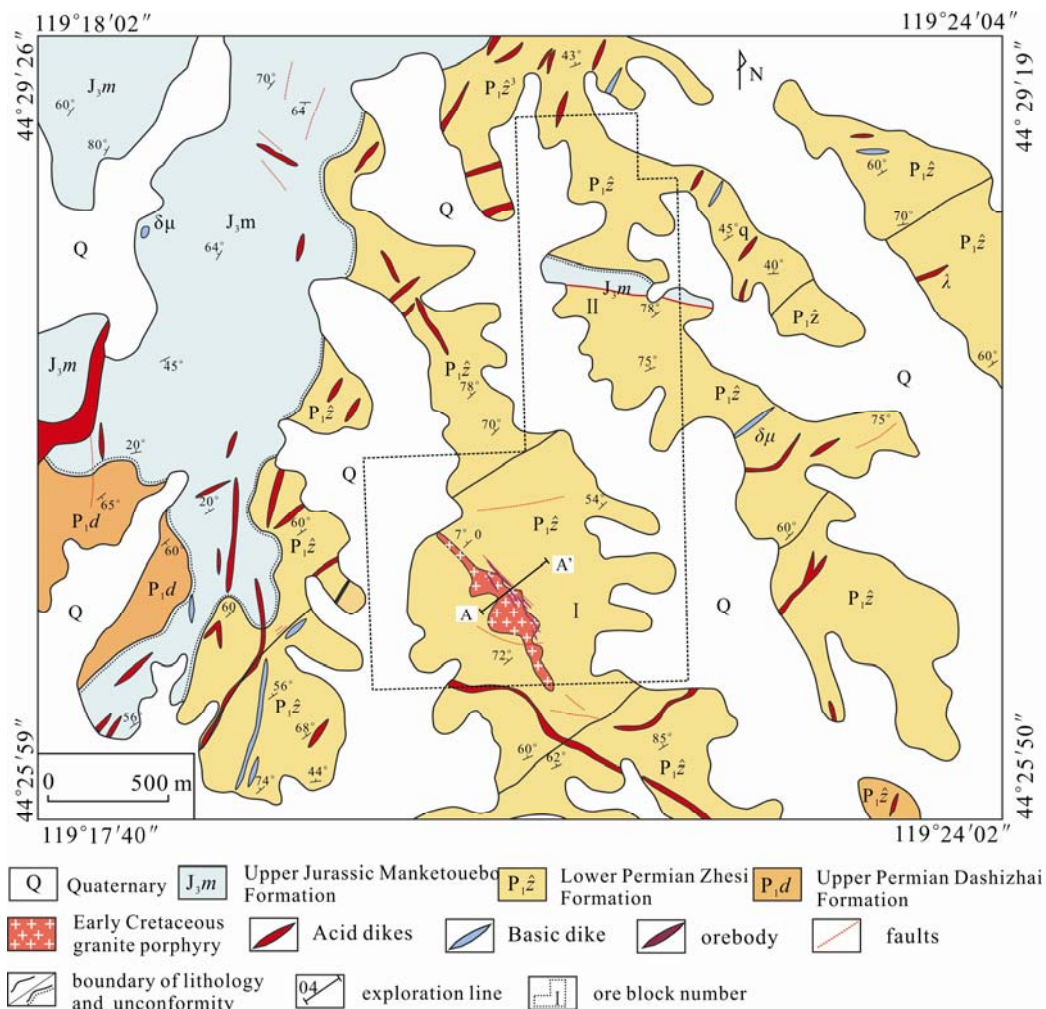


Fig. 5. Geological map of Dongshanwan deposit.

occurred in the deposit (Fig. 6).

3.2.2 Porphyry type mineralization in Haobugao area

In recent years, a series of work such as geological mapping, geochemical and geophysical exploration, trenching and drilling has been carried out in the periphery of the Haobugao mining area, and some polymetallic orebodies with characteristics of porphyry type mineralization have been discovered and evaluated in this area (Fig. 2). The ore minerals are commonly disseminated in the altered granite. Combined with the characteristics of mineral assemblages, ore textures and alterations, we believe that the mineralization in this area show characteristics of typical porphyry type deposit.

3.3 Hydrothermal vein type deposits

Hydrothermal vein type deposits, which occurred in different types of units, constitute another important type of ore deposits in SGXR (Fig. 7). The important hydrothermal vein type deposits in SGXR include Dajing Cu-Sn-Ag-Pb-Zn deposit, Bairendaba and Weilasituo Zn-Cu-Ag-Sn-W deposit and Shuangjianshan Pb-Zn-Ag deposit. Ore bodies of these deposits occur in specific Permian strata, and lack clear link with intrusive rocks in space and time. In recent years, geologists have tried to use different isotopic dating methods to study the formation ages of these deposits. Liao et al. (2014) carried out cassiterite LA-ICP-MS U-Pb isotope dating for the Dajing deposit and obtained the mineralization age of 144 Ma. Muscovite Ar-Ar dating conducted by Pan et al.

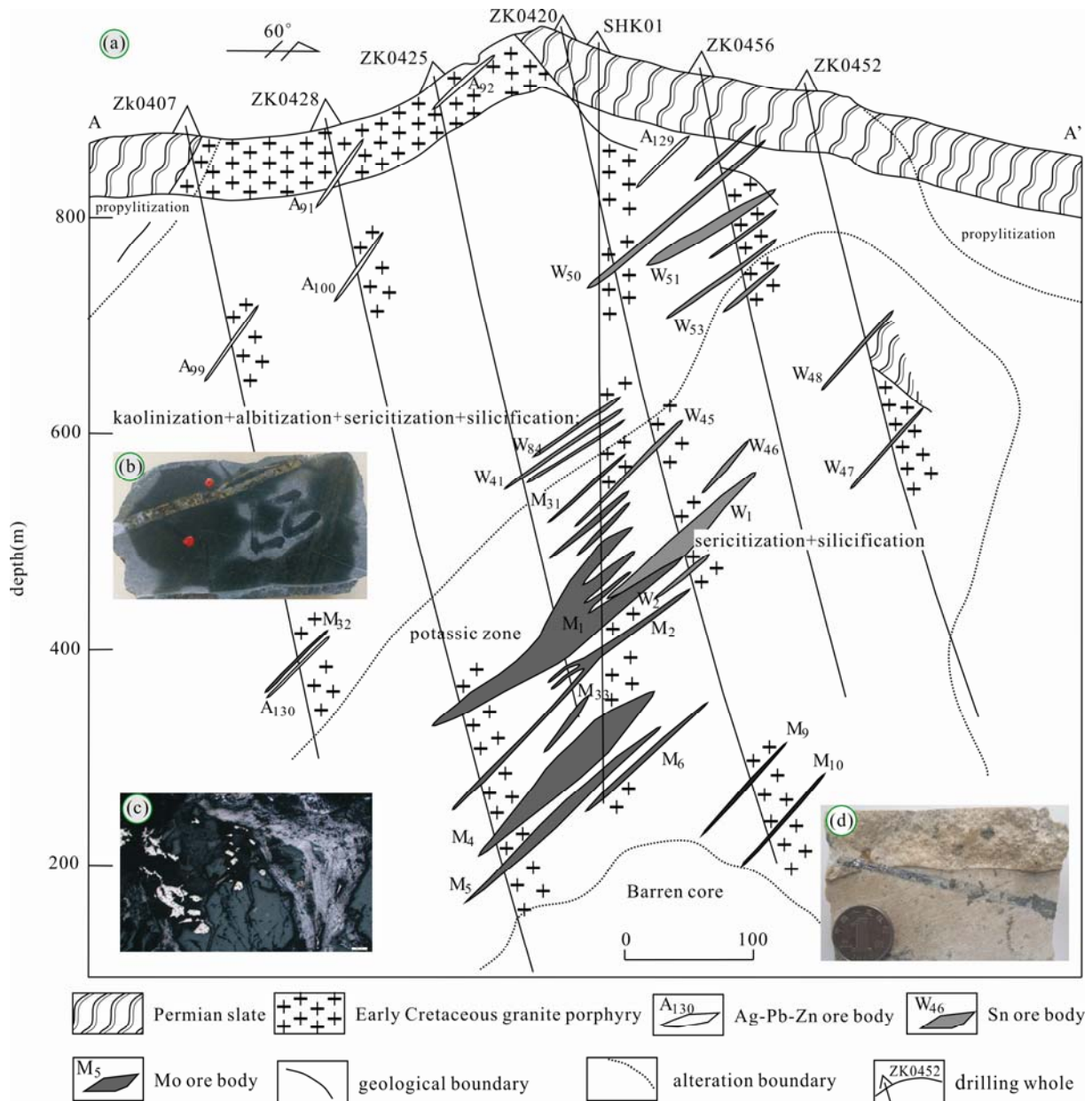


Fig. 6. (a) Cross-section of Dongshanwan deposit; (b) veinlet mineralization in Permian strata; (c) micrographs of Mo-bearing ores; (d) veinlet mineralization in granite

(2009) and Chang et al. (2010) reveals that the Weilasituo and Bairendaba deposit was formed at 133.4 Ma and 135.0 Ma, respectively. It can be concluded that the formation of hydrothermal vein type deposits in SGXR was also mainly concentrated in the Early Cretaceous Epoch.

3.3.1 Dajing deposit

The Dajing deposit is a large-scale Cu-Sn polymetallic deposit containing Cu, Sn, Zn, Pb, Ag and minor Ga, In. Ore-bearing strata of the Dajing ore deposit were the Upper Permian Linxi Formation. The Linxi Formation of this area can be divided into four sections from bottom to top: (1) black shale, (2) detrital rocks, (3) marls, and (4) vari colored detrital rocks. Four distinct fractures, extending in NE-, NW-, NWW- and NNW- directions, exposed in the mining area (Wang et al., 2015; Fig. 7b). NW-trending faults and the interlayer breccia form the main host structure for ore veins. The ore-hosting structures generally cut the strata with small angles ($< 20^\circ$) in the form of vein, network, composite vein and cross

vein (Wang et al., 2010; Fig. 8 a and c).

Three main kinds of ore types, including Cu-Sn-Ag ore, Pb-Zn-Ag ore and compound ore, exist in the Dajing mine. The main ore structures of the deposit include compact massive structure, brecciated structure, network structure, banded structure and strati form structure, and ore textures are various as granular, collo form, crush, poikilitic, exsolution, impregnation and metasomatic. Ore minerals in the deposit are originally composed of chalcopyrite, cassiterite, arsenopyrite, pyrite, galena, marmatite, pyrrhotite, acanthite. The major gangue minerals in ores are siderite, ankerite, calcite, quartz, sericite, chlorite, and fluorite (Fig. 9). Three main types of alteration were recognized in the deposit, namely, silicification, chloritization, carbonation (Wang et al., 2010). The deposit is formed by a multi-stage hydrothermal process, and hydrothermal veins with different mineral assemblages, including cassiterite-arsenopyrite-quartz, polymetallic-sulphides-quartz and polymetallic-sulphides-carbonate, developed in the mining

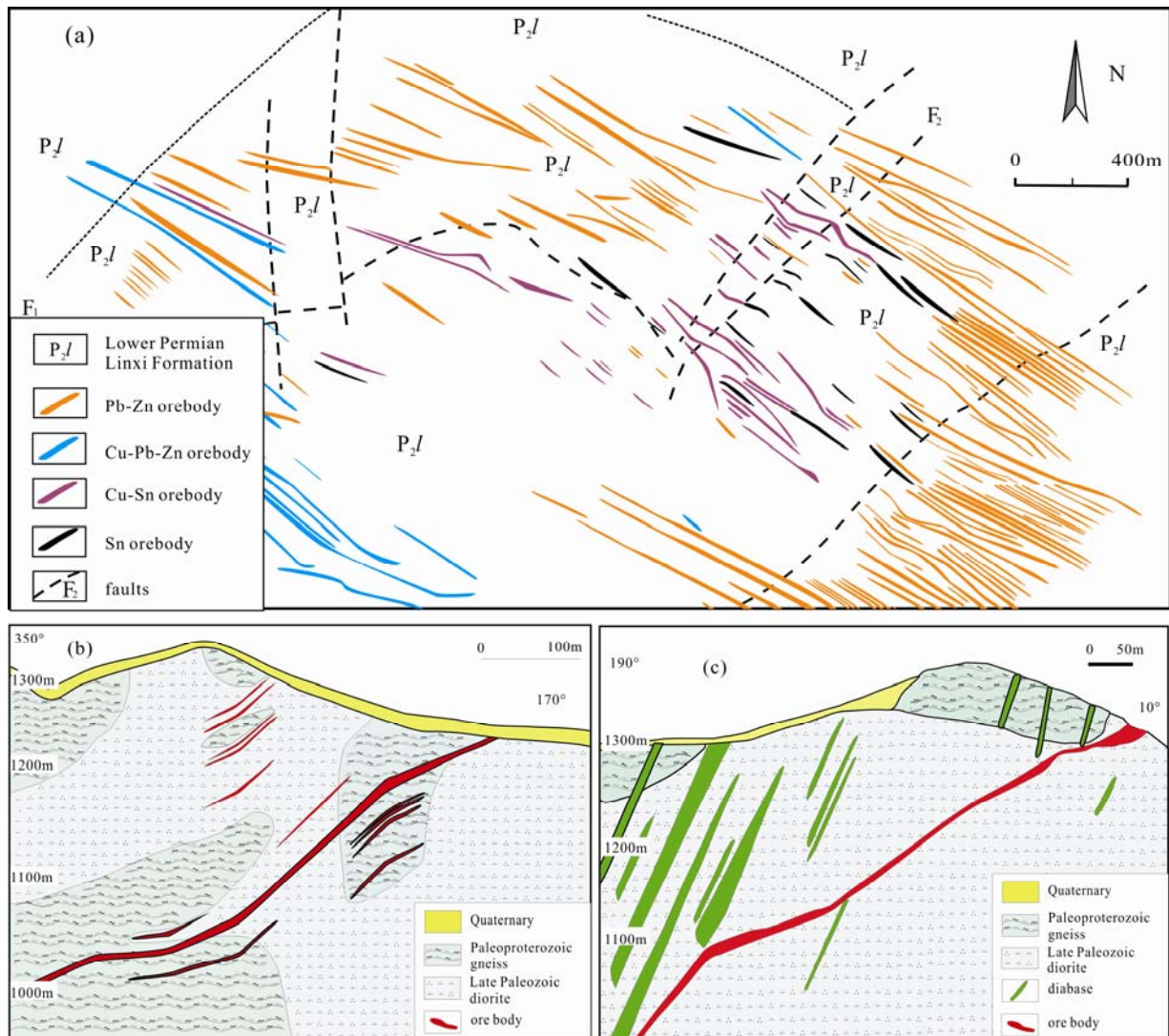


Fig. 7. Schematic map showing the vein type ore-bodies occurred in different geological units. (a) geological map of 600 meter level of Dajing deposit; (b) cross-section of the Bairendaba deposit; (c) cross-section of the Weilasituo deposit.

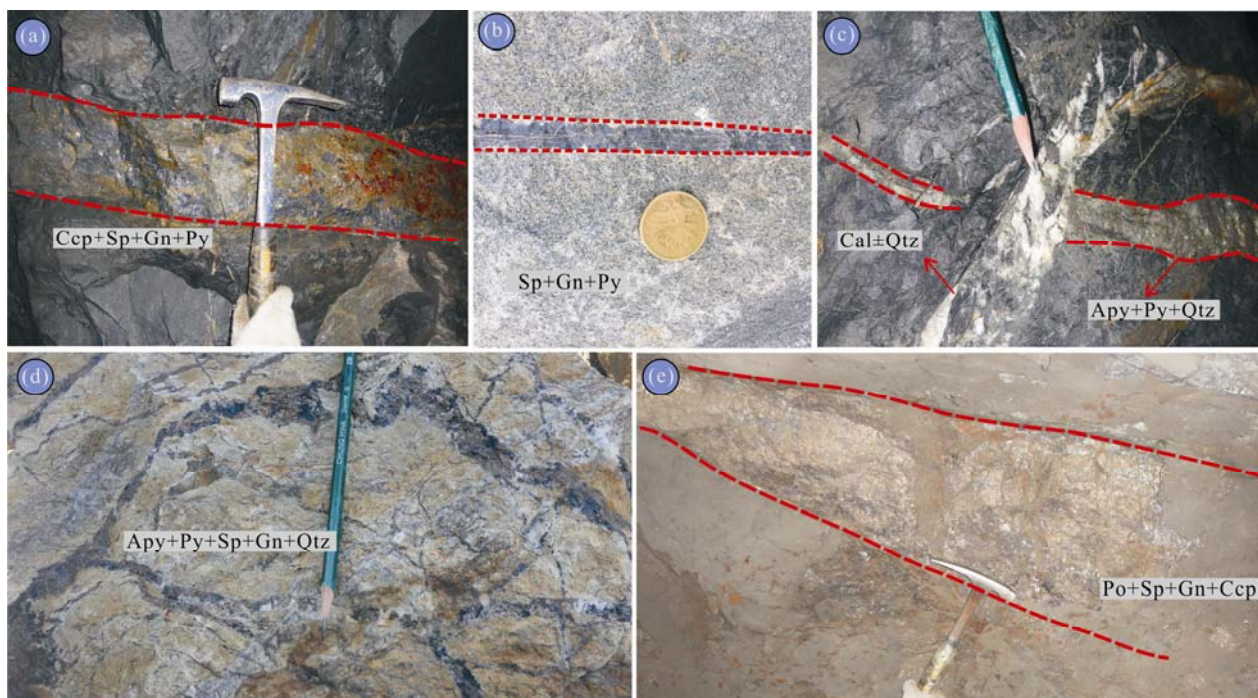


Fig. 8. Photos of ore-bodies and ores from hydrothermal vein type deposit in the SGXR.

(a) A vein type copper ore body (Dajing deposit); (b) veinlet polymetallic sulfide ores (Dajing deposit); (c) a carbonate vein cut crossarsenopyrite-quartz vein (Dajing deposit); (d) stockwork polymetallic sulfide ores (Bairendaba deposit); (e) a vein type copper-zinc orebody (Weilasituo deposit). Sp-sphalerite; Gn-galena; Py-pyrite; Ccp-chalcopyrite; Po-pyrrhotite; Apy-arsenopyrite; Qtz-quartz; Cal-calcite

area.

3.3.3 Bairendaba and Weilasituo deposits

The Bairendaba and Weilasituo deposits are located about 15 km apart, and both of them belong to mesothermal vein-type deposits controlled by fractures (Fig. 7c-d; Fig. 8g). The previous research reveals that the two deposits show similar characteristics, and are products of the same mineralization process (Jiang et al., 2010; Liu et al., 2014; Ouyang et al., 2015). The strata in the Bairendaba-Weilasituo area are relatively simple. The Xilinhote Complex is the oldest geological unit exposed in the mining area, and in addition to the Xilinhote Complex, another important geological unit in the mining area is Hercynian quartz diorite. The above two geological units also provide the main host rocks for mineralization (Jiang et al., 2010).

NE-, near EW- and NW- trending faults are developed in this area, and the nearly EW- trending fractures are major ore-control structures. Ore textures of this two deposits show typical characteristics of hydrothermal origin. And the structures of ores are common in banded, disseminated, massive and vein like structures. The ore minerals of this area show the following textures: euhedral, subhedral, and anhedral granular textures, exsolution texture, replacement textures (Fig. 8f-g). As a result of multi-stage hydrothermal activity, hydrothermal veins of different mineral assemblages are very developed in this area, and the most common veins include arsenopyrite-pyrite-quartz vein, polymetallic sulphide fluorite-(quartz)-(calcite) vein, sphalerite-pyrrhotite - chalcopyrite-fluorite vein, quartz calcite+ fluorite+

muscovite vein. Wall rock alteration in the Weilasituo and Bairendaba area is always developed along and adjacent to mineralized fracture zones. And the wall rocks of the orebodies are subjected to silicification and chlorite-carbonate alterations (Jiang et al., 2010).

4 Geochemistry

4.1 Fluid inclusions

Fluid inclusions in ore minerals reflect the physiochemical nature of the solutions present during the ore-forming process. In order to understand the property, evolution and source of ore-forming fluids of the deposits, we summarized the previous research on fluid inclusion petrography, microthermometry and Laser Raman of deposits from SGXR.

4.1.1 Types and assemblages of fluid inclusions

According to their phase composition at room temperature (25°C), phase transitions observed during heating and cooling, and Laser Raman spectroscopy, primary fluid inclusions of the three deposits can be divided into these following major types (Fig. 10; Table 2): (1) L-type (liquid-rich aqueous inclusions): The liquid-rich fluid inclusions consist of vapor and liquid water at room temperature, with $V_{H_2O}/(V_{H_2O} + L_{H_2O}) < 50$ vol. % (Fig. 10b and d). These fluid inclusions range in size from 5 to 25 μm and homogenize to liquid during heating; (2) V-type (vapor-rich inclusions): The vapor-rich fluid inclusions consist of vapor and liquid water, in which $L_{H_2O}/(V_{H_2O} + L_{H_2O}) < 50$ vol. %. These fluid inclusions occur in isolation or coexist with L- and S-type fluid

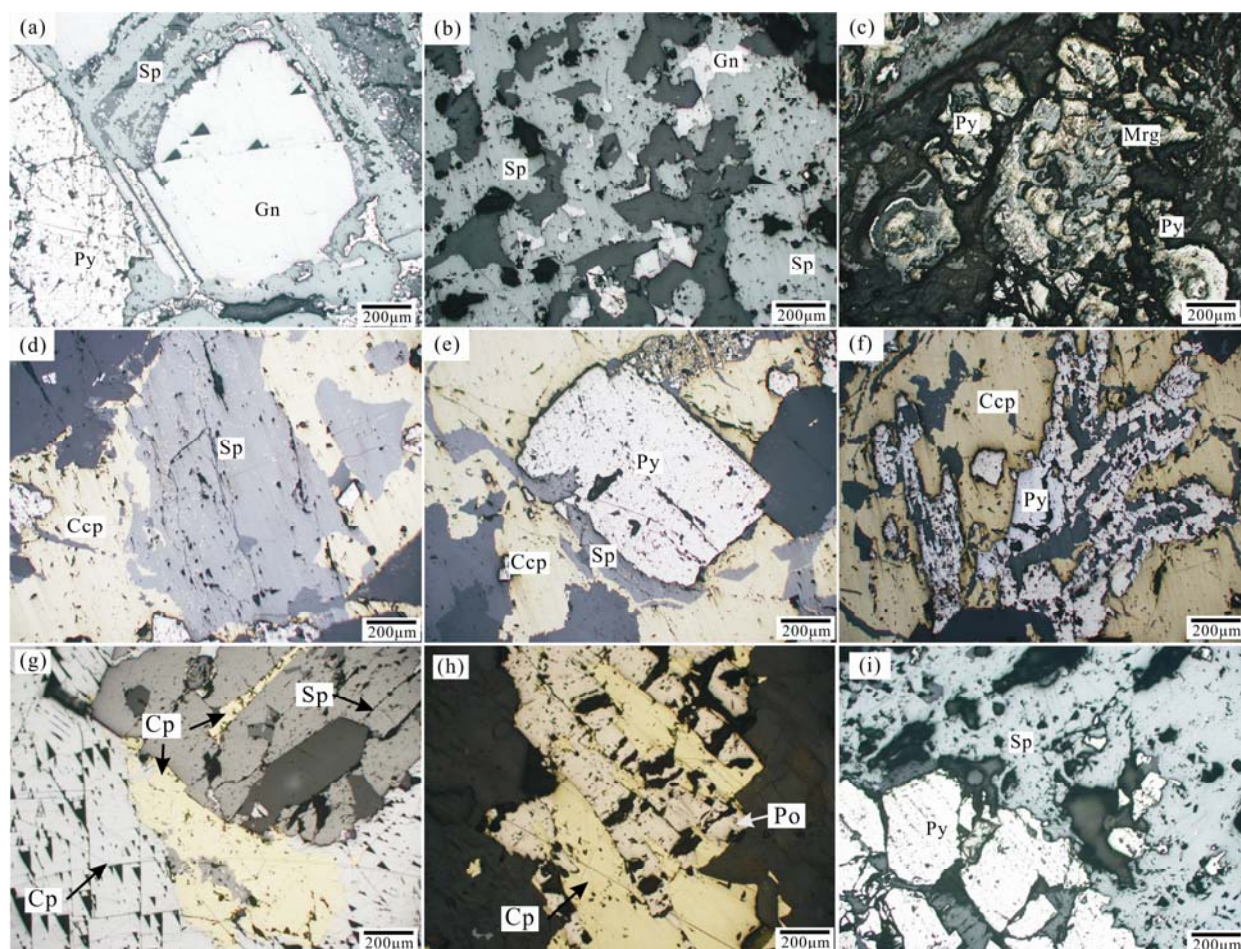


Fig. 9. Micro-photos of ores from hydrothermal vein type deposit in the SGXR.

(a) Rim texture, as the result of the edge of galena being replaced by sphalerite; (b) islanding galena, as the result of sphalerite being replaced by galena; (c) secondary changes of primary sulfide minerals; (d) exsolution texture (drop like chalcopyrite occurred in sphalerite); (e) Skeleton crystal textures, as the results of euhedral pyrite being replaced by sphalerite; (f) branch-like texture as a result of replacement along irregular fissure in pyrite; (g) chalcopyrite replaced sphalerite and galena along their contact zone; (h) pyrrhotite was replaced by chalcopyrite along its cleavage; (i) islanding pyrite residues in sphalerite; Sp- sphalerite; Gn- galena; Py- pyrite; Ccp- chalcopyrite; Po- pyrrhotite.

Table 2 Summary of fluid inclusion assemblages of Early Cretaceous deposits from Southern Great Xing'an Range

Name of deposit	Mineralization stage	Host mineral	Fluid inclusion type	Homogenization temperature °C	Reference
Haobugao	Mineralized granite	Quartz	S,V,L	286–432	Our previous study
	Early	Garnet	S,V,L	329–421	
	Middle	Quartz	V,L	308–440	
	Late	Calcite/ fluorite	L,C2	145–265	
Huanggang	Mineralized granite	Quartz	L,V,S	290–434	Our previous study
	Early	Garnet	L,V,S	235–387	
	Middle	Quartz	L,V,S	254–484	
	Late	Calcite	L,C1	183–293	
Dongshanwan	Mineralized granite	Quartz	L,V,S	203–498	Our previous study
	Early	Quartz	L,V	299–322	
	Middle	Quartz	L,V	201–353	
	Late	Quartz	L	199–274	
Dajing deposit	Disseminated orebody	Quartz	S,L,V	134–462	Li et al., 2015
	Vein type orebody	Quartz/ fluorite	L,V	150–240	
Bairendaba	Early	Quartz	L	262–374	Ouyang, 2013
	Middle	Quartz/ Fluorite /calcite	LC1	366–384	
	Late	Quartz calcite	L		
Weilasituo	Early	Quartz	V,L,C1	242–400	Quan et al., 2017
	Middle	Quartz	L,C2	190–331	
	Late	Quartz	L	180–241	

L-liquid-rich aqueous type inclusions; V-vapor-rich type inclusions; S- daughter-mineral-bearing three-phase type inclusions; C₁- CO₂-bearing inclusions; C₂- CH₄-rich inclusion

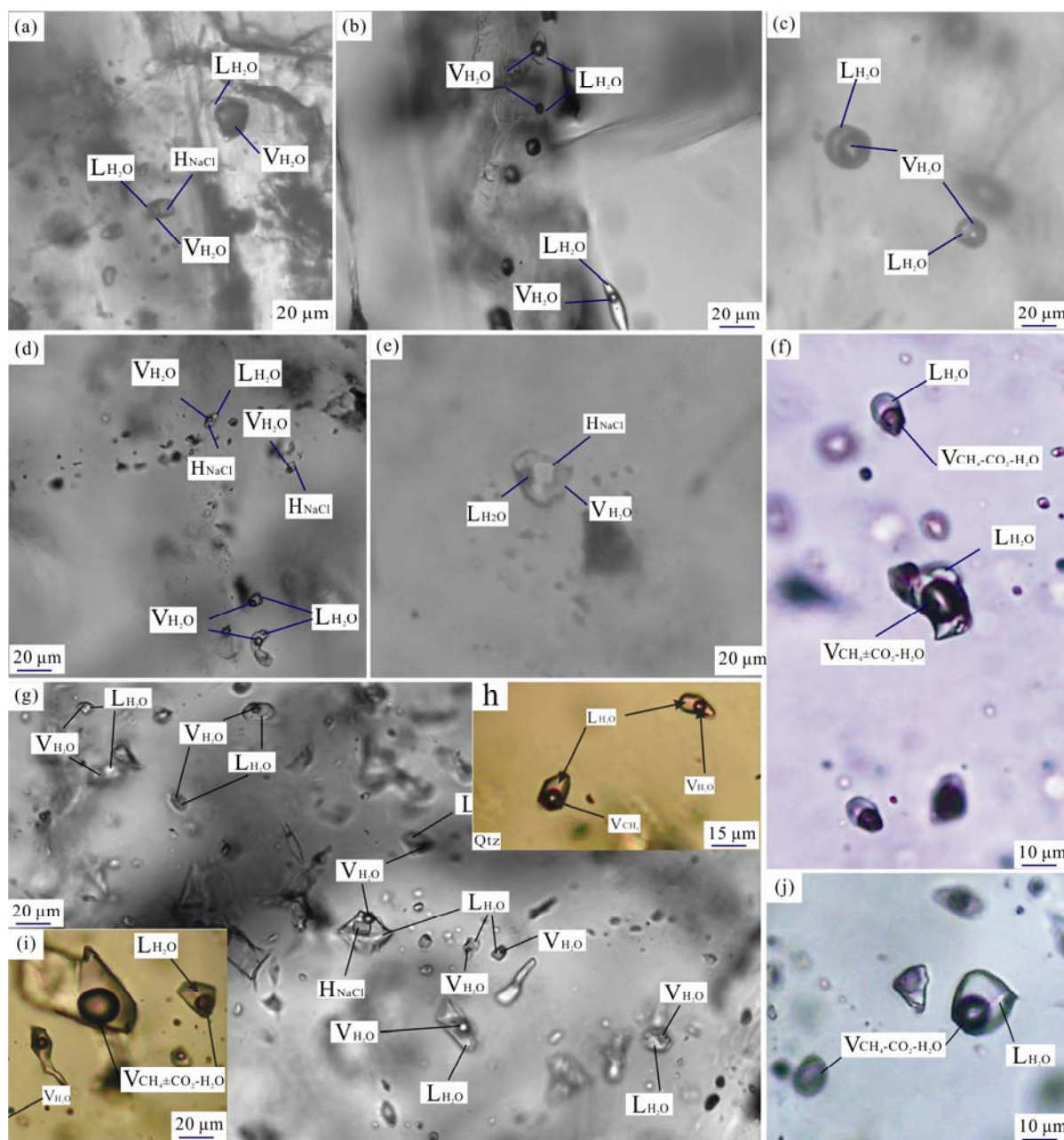


Fig. 10. Representative microphotographs of fluid inclusions in ores of deposits mentioned in the paper.

(a) L-type fluid inclusions coexists with V-Type and S-Type fluid inclusions in garnet of skarn stage (Haobugao deposit); (b) an L-Type inclusion coexists with a V-Type inclusion in garnet (Huanggang deposit); (c) L-Type fluid inclusions coexist with S-Type fluid inclusions in garnet; (d) L-Type fluid inclusions in garnet (Huanggang deposit); (e) an S-Type fluid inclusion in quartz (Haobugao deposit); (g) S- type fluid inclusion coexisted with VL- type fluid inclusions of (Dajing deposit); (f), (j) C₁-type inclusions in ores from the Bujinhei deposit; (i), (h) C₂-type inclusions in ores from the Weilasituo deposit; L-type: liquid-rich aqueous inclusions; V-type: vapor-rich inclusions; S-type: daughter-mineral-bearing three-phase inclusions; C₁-type: CO₂-bearing inclusions; C₂-type: CH₄-rich inclusions.

inclusions and homogenize to vapor during heating (Fig. 10a and c); (3) S-type (daughter-mineral-bearing three-phase inclusions): S-type inclusions contain a vapor bubble, an aqueous liquid, and one or several solid daughter minerals at room temperature. The S-type inclusions are typically present in garnets of skarn type deposits, quartz phenocrysts of intrusions from porphyry type deposit can also find this type of fluid inclusions. In these deposits, the solid daughter minerals are mainly

angular cube shapes, and they were identified as halite by their microscopic characteristics (Fig. 10e, g). Besides, the hydrothermal vein type Dajing deposit also developed S-type fluid inclusions, but the numbers and types of daughter minerals are different from other ore deposits; (4) C₁-type (CO₂-bearing inclusions): The CO₂-bearing inclusions consist mainly of two components—an aqueous solution and CO₂ (Liquid CO₂ + Gaseous CO₂). This type of fluid inclusions can be identified in calcites from

Huanggang deposit and Weilasituo deposit; (5) C₂-type (CH₄-rich inclusion): The C₂-type inclusions generally occur as two phases consisting of an aqueous liquid and a carbonic vapor with varying phase ratios of between 60 and 90 vol.% at room temperature. They occur as isolated cavities in healed microfractures in fluorite of Haobugao, Weilasituo and Bairendaba deposit (Fig. 10f, h–j). Laser Raman revealed these inclusions are CH₄-dominated, with variable proportions of N₂ and CO₂ (Fig. 11).

For porphyry and skarn deposits, the fluid-inclusion assemblage of ores experienced a similar evolution process from early to late mineralization stage, namely, Type-V + Type-L + Type-S → Type-V + Type-L ± (Type-C₁) ± (Type-C₂) → Type-L ± (Type-C₁). Halite-bearing fluid inclusions (Type-S) and vapor-rich fluid inclusions (Type-V) coexist in minerals of skarn and porphyry type deposits, indicating that primary fluid inclusions of the two types of deposits were captured almost simultaneously when the fluids were boiling (Roedder, 1971; Lu et al., 2004; Ni et al., 2015). With the change of fluid inclusion assemblages, homogenization temperatures and salinities of the deposits all tended to decrease dramatically, indicating that the ore forming fluids changed from a boiling hydrothermal NaCl–H₂O ± (CH₄–CO₂) system to a homogeneous NaCl–H₂O system.

For hydrothermal vein type deposits, significant differences appeared in fluid inclusion assemblages of different deposits. The ores from Weilasituo and Bairendaba deposit mainly develop liquid rich two-phase (L-Type), CH₄-rich two phase (C₂-Type) and CO₂–(CH₄)-bearing three phase (C₁-Type) inclusions, indicating that the ore forming fluids of the deposit belong to a complex NaCl–H₂O–CH₄–CO₂ system. The fluid inclusion assemblages of the Dajing deposit are characterized by occurrence of daughter mineral-bearing type (S-type) inclusions which is quite different from other hydrothermal vein type deposits. The S-type inclusions are prominent, in which abundant daughter minerals are contained, and sometimes a single inclusion may contain as much as 4–5 daughter minerals. And these daughter mineral-bearing S-type fluid inclusions are generally

coexisted with L-type and V-type fluid inclusions (Wang, 2000).

4.1.2 Salinities and homogenization temperatures of fluid inclusions

Homogenization temperatures of fluid inclusions from Early Cretaceous deposits are highly varied, but the main stage of mineralization interval corresponds with the medium-temperature (around 180–300°C). Fluid inclusions of early-stage, which are more likely represent fluids before lead-zinc mineralization, tend to show higher homogenization temperatures than the middle and late-stage fluids. Generally, homogenization temperatures of early-stage fluid inclusions are mainly in the 290–420°C range for skarn type deposits, 230–320°C range for porphyry type deposits, and 240–330 °C range for the hydrothermal vein type deposits. For skarn and porphyry deposits in the study area, daughter-bearing mineral inclusions of high salinity appeared in the early stage of mineralization. Salinities of these salt-bearing fluid inclusions are commonly more than 35 wt% NaCl eqv. whereas salinities of daughter mineral-absent fluid inclusions typically lower than 12 wt% NaCl eqv. As the only hydrothermal vein type deposits which is dominantly by Sn–Cu mineralization, the Dajing deposit also developed daughter-bearing mineral inclusions, indicating that the metallogenic conditions and genetic mechanism of this deposit are different from other deposits of similar types. Fluid inclusion microthermometry constrains temperature intervals of approximately 180 to 400°C and 262 to 384°C for Weilasituo and Bairendaba stage, respectively (Ouyang, 2013; Quan et al., 2017). And ore forming fluids in the main-ore stage of this two deposit are characterized by low-salinities (<9 wt% NaCl eqv.; Ouyang et al., 2014).

4.1.3 Composition of fluid inclusions

The results of laser-Raman spectroscopic analysis indicate that: (1) For skarn type deposits (Huanggang and Haobugao), gas and liquid components in fluid inclusions of skarn minerals is dominated by H₂O, whereas that of

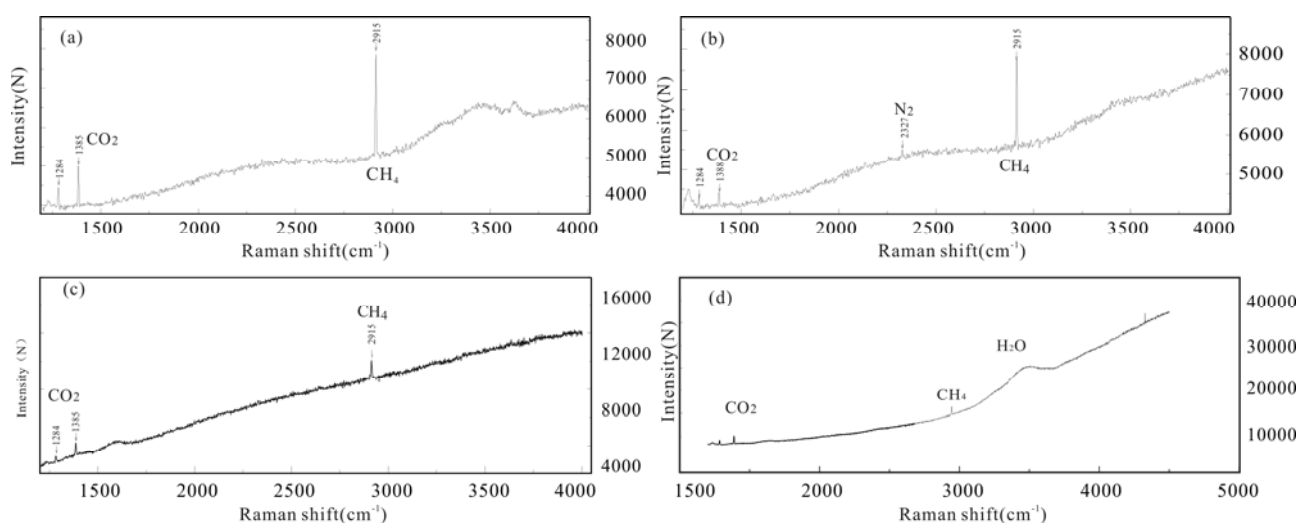


Fig. 11. Laser Raman Evidence of Carbonaceous Fluid Participation in Mineralization. (a) Haobugao; (b) Weilasituo deposit; (c) Bujinhei deposit; (d) Haobugao deposit.

mineral in quartz-sulfide stage contains a certain amount of CH₄ and CO₂. (2) As stated above, CH₄ and CO₂ are identified in vapor bubbles of two phases fluid inclusion in skarns of Haobugao and Huanggang deposit by laser Raman, but CO₂-bearing three phases fluid inclusions were not observed at room temperature and during freezing in this study, thus CO₂ only occurs as a minor component (<3.5 mol%) that is considered as insignificant in regards to the bulk composition of the hydrothermal fluids (Azbej et al., 2007). (3) For hydrothermal vein type Weilasituo and Bairendaba deposit, vapor bubbles of vapor-rich inclusions contain variable CO₂ and CH₄ contents and rare N₂ concentrations in ores of early stage and liquid and vapor compositions of fluid inclusions are mainly composed of H₂O (Fig. 11). And with the formation of the ore, carbonaceous components in fluids presented as an increased at first and then decreased trend from the early to late stages.

4.2 Isotope geochemistry

4.2.1 Hydrogen and oxygen isotope

Hydrogen and oxygen isotopes have been measured on a variety of minerals and some inclusion fluids from deposits of SGXR. In this paper, we organized the hydrogen and oxygen isotope data obtained by our and predecessors' research, and the oxygen isotope values of ore-forming fluids are also re-estimated based on the latest microscopic thermometric data of fluid inclusions (Table 3). On a δD vs. $\delta^{18}O_{H_2O}$ diagram (Fig. 12a), data points of garnets from Haobugao and Huanggang deposits fall below the magmatic water field, indicating that the initial ore-forming fluids of skarn type deposits were mainly derived from magmatic fluids (Zhou et al., 2011). Data points of the Weilasituo, Bairendaba and Dajing deposit plot in the lower-left part of the magmatic water field, which is obviously shifting toward the meteoric water line (Feng et al., 1994; Liu et al., 2003; Ouyang, 2013). In particular, some of the deposits, like Dongshanwan, have relatively lower hydrogen isotope values, the hydrogen isotopes values of some samples are even lower than that of Mesozoic meteoric water which is estimated by Ma et al. (2008).

4.2.2 Sulfur isotope

The Early Cretaceous hydrothermal deposits in the study area have similar sulfur isotopic compositions which are characterized by narrow changing ranges. Table 4 and Fig. 12b present the sulfur and lead isotopic compositions of ore minerals obtained from previous studies (Zeng et al., 2009; Shao et al., 2010; Zhou et al., 2012). The $\delta^{34}S$ values of sulfide samples (galena and sphalerite) from the Haobugao deposit varied between -2.7‰ and -0.9‰, with a mean value of -1.6‰. The $\delta^{34}S$ values of sulfides from the Huanggang deposit generally ranged from -9.5‰ to 4.5‰. The mean $\delta^{34}S$ values of molybdenite, sphalerite, and chalcopyrite are -0.13‰, -2.00‰, and -2.61‰, respectively. The $\delta^{34}S$ value of ore minerals from Bairendaba and Weilasituo deposit vary from -3.6 to 1.7‰ and 9.4 to 2‰, with peak values of -2.0 to -1.0‰ and -4.0 to 2.0‰, respectively (Jiang et al., 2010). The

$\delta^{34}S$ values of sulfides in the Dajing deposit also have a relatively narrow range between -1.8 to ~3.4‰, which are similar to those of the other hydrothermal vein type deposits (Fenget al., 1994; Chu and Huo, 2002; Liu et al., 2003; Niu et al., 2008; Chu et al., 2010).

4.2.3 Lead isotopes

The lead isotopic compositions of the ore samples from the Early Cretaceous deposits of SGXR were also characterized by a limited variation in $^{206}Pb/^{204}Pb$, $^{207}Pb/^{204}Pb$, and $^{208}Pb/^{204}Pb$. And lead isotope compositions of ores from same type of deposits show similar characteristics (Fig. 13). The $^{206}Pb/^{204}Pb$, $^{207}Pb/^{204}Pb$, and $^{208}Pb/^{204}Pb$ ratios of the skarn type deposits ranged from 18.248 to 18.279, 15.488 to 15.634 and 37.927 to 38.436, respectively, which was close to feldspars of the Early Cretaceous granites (Zhou et al., 2012; Li, 2015). The mean values of $^{206}Pb/^{204}Pb$, $^{207}Pb/^{204}Pb$, $^{208}Pb/^{204}Pb$ ratios of Weilasituo, Bairendaba, and Dajing deposit were 18.326, 18.366, 18.304, 18.282 and 15.553, 15.571, 15.525, 15.538, and 38.237, 38.313, 38.046, 38.241, respectively (Chu and Huo, 2002; Ouyang et al., 2014).

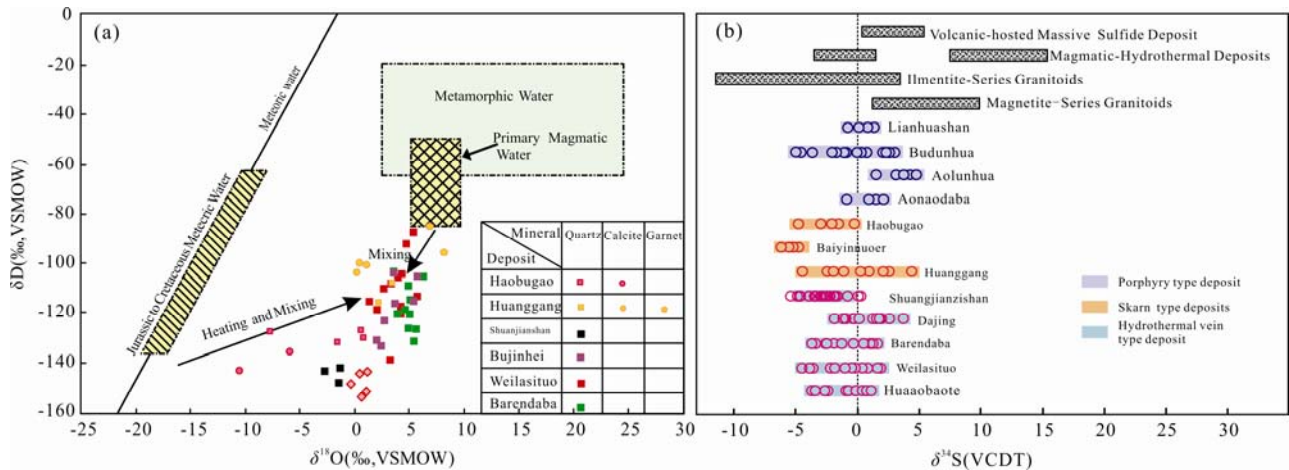
5 Discussion

5.1 Sources of ore-forming fluids

Some features of the ore forming hydrothermal system at the Early Cretaceous deposits of SGXR can be inferred from the fluid inclusion and isotope geochemistry data. As described above detailed observation of the skarn and porphyry deposits from SGXR yielded three types of inclusions: Type-S, Type-V, and Type-L. The coexistence of fluid inclusions with similar homogenization temperatures but contrasting salinities is interpreted as evidence of boiling in the ore-forming hydrothermal system (Roedder and Bodnar, 1980). It is generally believed that this kind of ore-forming fluid can be directly derived from the magma differentiated hydrothermal solutions (Cline, 1994). Fluid inclusion of quartz phenocrysts is considered to be earliest record of fluids exsolved from an igneous intrusion (Harris et al., 2003; Vasyukova et al., 2008). By comparing fluid inclusion in ores and hosting granites, we noted that the types of fluid inclusions in ores of early stage are consistent with quartz phenocrysts of granite. This further proves that the initial ore-forming fluids of skarn and porphyry type deposit might be derived from magmatic hydrothermal activities. The H-O isotopic compositions of early stage from skarn type deposits are consistent with fluids derived from magmatic sources, indicating that the initial ore forming fluids show a close genetic relationship between magmatic differentiation hydrothermal solutions (Taylor, 1997). As for other types of deposits, the majority of $\delta^{18}O_{H_2O}$ values of main mineralization stage were between meteoric water and primary magmatic water, suggesting that the ore-forming fluid could be mixed with significant meteoric water during its evolution. In addition, we also noted that the Early Cretaceous hydrothermal deposits in SGXR have very lower hydrogen isotope values, and the hydrogen isotope levels of some deposits are even lower than

Table 3 List of Hydrogen and Oxygen Isotope Compositions of Early Cretaceous deposits from Southern Great Xing'an Range

Ore deposit	Mineralization stage	Mineral	$\delta^{18}\text{O}_{\text{Q-SMOW}}/\text{‰}$	$\delta\text{D}_{\text{H}_2\text{O-SMOW}}/\text{‰}$	$\delta^{18}\text{O}_{\text{H}_2\text{O-SMOW}}/\text{‰}$	References
Haobugao	Middle	Quartz	5.7~5.9	-130.5~-127.3	2.45~2.65	Our previous study
	Late	Quartz	-2~4.1	-132.2~-125.5	-7.58~-1.48	
	Late	Calcite	-4.8~-0.5	-144.1~-136.0	-14.34~-9.04	
Huanggang	Early	Garnet	6.2~7.8	-96~-83	7.4~9.1	Zhou et al. 2011
	Middle	Quartz	9.5~10.6	-116~-108	4.5~4.9	
	Late	Calcite	5.7~6.6	-104~-101	-2.8~-3.8	
Dajing	Early	Quartz	13.36	/	7.15	Feng et al., 1994; Liu et al., 2002;
	Early	Cassiterite	2.06~1.52	/	4.51~4.58	
Bairendaba	Early	Quartz	11.99~14.24	/	-0.38~-2.57	Ouyang., 2013;
	Early	Quartz	15.2~15.4	-100.9~-108	10.45~10.65	
	Middle	Quartz	11.6~16.5	-132.0~-104.0	3.31~6.01	
	Middle	Fluorite		-130.2~-106.4	5.32~7.12	
	Late	Calcite	12.04~13.69	-120.3~-104.6	6.94~8.59	
Weilasituo	Late	Fluorite		-83~-75	-15.8~-5.2	Ouyang, 2013; Wang et al., 2010
	Late	Calcite	-1.36~10.29	-90.1~-74.5	-16.06~-4.41	
	Late	Quartz	12.25~16.63	-139.4~-88.2	1.15~5.5	

**Fig. 12.** Calculated H-O isotopic composition of fluids responsible for ore deposits in the SGXR (a); Sulfur isotope compositions of sulfide minerals from Early Cretaceous deposits in SGXR (b).

The data are from Feng et al., 1994; Chu and Huo, 2002; Liu et al., 2002; Niu et al., 2009; Zeng et al., 2009; Jiang et al., 2010; Zhou et al., 2011; Zhou et al., 2012; Ouyang, 2013; Ouyang et al., 2014; Li et al., 2015; Wang, 2017; Zhang, 2018).

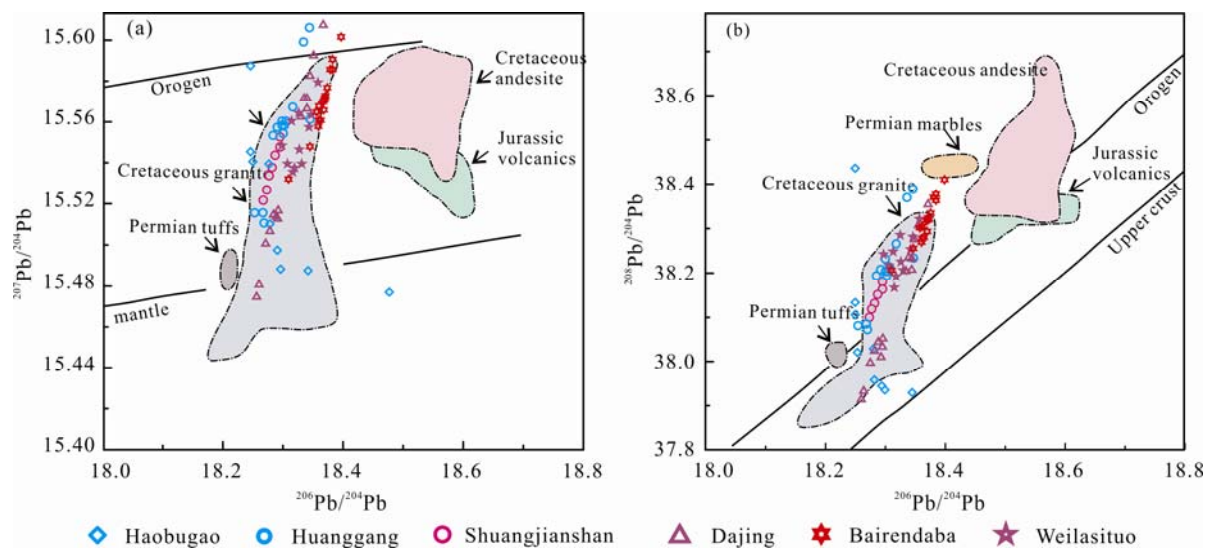


Fig. 13. $^{207}\text{Pb}/^{204}\text{Pb}$ vs $^{206}\text{Pb}/^{204}\text{Pb}$ (a) and $^{208}\text{Pb}/^{204}\text{Pb}$ vs $^{206}\text{Pb}/^{204}\text{Pb}$ (b) diagrams of sulfides, Cretaceous granite, and esite and major geological units of SGXR (modified after Zhai et al., 2014, the data are from Ouyang et al., 2014; Zhai et al., 2014; Li et al., 2015; Jiang et al., 2017)

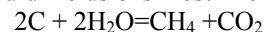
Table 4 Sulfur isotope compositions of sulfide minerals of Early Cretaceous deposits from Southern Great Xing'an Range

Name of deposit	mineral	Range (‰)	Average(‰)	Extreme difference range	Number of samples	Reference
Haobugao	Galena	-2.7~-2.3	-2.33	0.4	3	Our previous study
	Sphalerite	-1.6~-0.9	-1.3	0.7	3	
	Chalcopyrite	-1.6~-1.1	-1.3	0.5	3	
Huanggang	Molybdenite	-9.5~-4.5	-0.13	14	6	Zhou et al. (2012); Zeng et al. (2009)
	Arsenopyrite	-1.0~-2.2	0.53	3.2	3	
	Chalcopyrite	-6.7~-1.1	-2.61	7.8	10	
	Sphalerite	-9.0~-2.5	-2	11.5	13	
	Galena	-0.8~-0.3	-0.55	0.5	2	
Dajing	Arsenopyrite	1.5~3.4	2.43	1.90	4	Feng et al., 1994; Liu et al., 2002 Niu et al., 2009; Chu and Huo, 2002;
	Pyrite	-0.9~-2.1	0.78	3.00	18	
	Chalcopyrite	-0.2~-1.7	1.02	2.10	9	
	Sphalerite	-1.8~-2.6	1.26	4.40	12	
	Galena	-1.1~-1.8	0.30	2.90	3	
Bairendaba	Arsenopyrite	0.6~+1.7	1.0	0.9	3	Ouyang, 2013 Jiang et al., 2010
	Sphalerite	-1.6~-1.3	-0.56	2.9	15	
	Galena	-3.6~-2	-2.2	1.6	17	
	Pyrrhotite	-2.4~-0.5	-1.38	1.9	9	
Weilasituo	Sphalerite	-9.4~-2		11.4	19	Ouyang, 2013 Jiang et al., 2010
	Pyrite	-1.8~-0.4		2.2	6	
	Galena	-3.8~-3.5	0.3	3.7	2	
	Pyrrhotite	-1.0~-0.2	-0.5	1.2	5	
	Arsenopyrite	-0.5~-1.2	0.7	1.7	4	

Mesozoic meteoric water. Obviously, such a lower hydrogen isotope value of ore forming fluids is beyond what can be explained by precipitation of meteoric water. The hydrogen of organic matter in the sedimentary strata usually has a lower value. Therefore, we believe that the reaction between ore-bearing fluids and organic-rich country rocks may be the main reason for the relatively depleted δD fluids isotopic compositions of ore forming fluids.

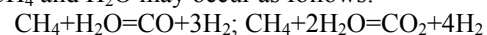
One of the important features the Early Cretaceous deposits is that the appearance of carbonaceous components in ore-forming fluids (mainly including CH_4 and CO_2). The reducing gas, including CH_4 and CO_2 , is not very common in hydrothermal metallogenic system but in metamorphic fluids (Rowins, 2000; Xu et al., 2007). There exist many different explanations for the genesis of this type of fluids, such as magma origin, decomposition of organic matter in strata and decarbonization of calcium silicate rocks (Kerkhof and Thiéry, 2001; Fan et al., 2004; Xu et al., 2009). Over the past years, especially, with the introduction of the concept of reduced porphyry type deposits, scholars gradually realize that carbonaceous composition is also an important part of ore-forming hydrothermal solution. CH_4 and CO_2 have also been detected in fluid inclusions from Huanggangliang, Haobugao, Weilasituo deposit by previous researches, and these gas compositions of mineral inclusion are also considered to be derived from deep seated magma (Zhou et al., 2011; Ouyang et al., 2014). However, thermal degradation of organic material from strata also can result in the generation of CH_4 and CO_2 (Ague, 1988; Rowins, 2000). Silty slate, silty mudstone, carbonaceous slate and other organic-rich rocks are very developed in the Permian Dashizhai Formation and Linxi Formation, the above strata are also constitute the main ore bearing strata of the Early Cretaceous hydrothermal deposits in the study area. We therefore

conclude that CH_4 in ore-forming fluids of the deposits may be products of dehydroxylation of organic carbon in the Permian strata. And CH_4 and CO_2 contained in the fluid inclusions most likely formed by the reaction



between carbonaceous slate from Permian strata and hydrothermal fluids during migration.

More importantly, thermal decrepitation is the most frequently used method of extracting fluid inclusions for stable isotope analysis (Coleman et al., 1982). For this method, the water (H_2O) in the fluid inclusions was extracted by decrepitation of quartz grains at $500^\circ C$, and hydrogen (H_2) was obtained by reduction of the collected water (H_2O) with Zn shot at $450^\circ C$. In this process, chemical reaction and isotope exchange between CH_4 and H_2O may occur as follows:



Therefore, the existence of CH_4 -rich fluid inclusions and isotope exchange between methane (CH_4) and water (H_2O) at high temperatures may dramatically affect the measured hydrogen isotope values of water (H_2O) in the fluid inclusions. And the appearance of CH_4 -rich fluid inclusions could be also an important reason for the quite lower hydrogen isotope values of the collected water from fluid inclusions. The CH_4 components of fluid inclusions probably came from dehydroxylation of organic carbon and fluids wall rock reaction.

5.2 Source of ore-forming materials

Generally, the ore-forming materials of hydrothermal deposits can be derived from the following possible sources: (1) Magmatic materials carried by deeply-derived fluids; (2) Materials extracted from sedimentary or metamorphic wall rocks; or (3) mixtures of the above two sources. Sulfur-lead isotopes are commonly used to constrain the source of the ore-forming materials, and we collected the sulfur and lead isotope data of minerals from

the Early Cretaceous hydrothermal deposits in the study area.

The total sulfur isotopic composition of the hydrothermal system is a function of the physicochemical conditions including temperature, pH value, oxygen fugacity and ion activity (Ohmoto and Rye, 1979; Hoefs, 1997). Therefore, average $\delta^{34}\text{S}$ of sulfide minerals that formed in hydrothermal systems can only represent the origin of ore-forming materials to some extent. As previously described, the $\delta^{34}\text{S}$ values of samples from skarn porphyry and hydrothermal vein type deposit ranged from -6.5 to $+5.0$, -5.0 to $+5.0$ and -5.5 to $+9.0$, respectively. The $\delta^{34}\text{S}$ values for the deposits are characterized by close to magmatic sulfur, and are distinctly different from that of the host sedimentary rocks (Fig. 12b). These observations suggest that the deposits mentioned in paper can be interpreted to reflect a magmatic source for the sulfur, and formations of these deposits are controlled by the Early Cretaceous intrusions.

It is generally believed that the lead derived from the same source should show similar Pb isotope compositions and variation trends, while Pb isotope compositions of different geological units are quite different. The host rocks of the Early Cretaceous deposits in the study area mainly include Permian low grade metamorphic detrital rocks, marble, Paleozoic gneiss and Hercynian granites. As illustrated in Fig. 13, the Pb isotopic compositions of the Early Cretaceous hydrothermal deposits are remarkably similar, and Pb isotopic compositions of sulfides are consistent with Early Cretaceous intrusions. We therefore infer that the Early Cretaceous magmatism could have been the most significant source of lead in the ores.

5.3 Genetic types of the deposits

Controversy on the the genesis and formation mechanism of skarn-related deposits from SGXR has never stopped in academia. Two representative views on the genesis of skarn deposits exist in academia: hydrothermal metasomatic origin and exhalative sedimentary origin. For a long time, the skarn-related deposits in the study area are recognized as the origin of Permian exhalative sedimentation. The evidence is mainly focused on the characteristics of stratiform and stratoid ore bodies which occur in Permian strata (Liu et al., 2001; Ye et al., 2002, Wang et al., 2007; Zeng et al., 2007). There are also some other scholars have proposed that the skarn in SGXR is of magmatic-hydrothermal origin, and their evidence mainly includes the following three aspects: (1) Daughter-mineral bearing fluid inclusions were found in some mineralized skarn minerals, and the occurrence of melt inclusions were regard as one of the major evidences of magmatic origin (Wang et al., 2010; Mei et al., 2015). (2) Systematic geological survey proved that different types of hydrothermal minerals, such as quartz, calcite and fluorite, are very developed in ores. These minerals, constitute different types of veins, or occur as cements in breccias type ores. (3) More importantly, the existence of mineralization and alteration within Mesozoic intrusions has been proved, these discoveries have undoubtedly added direct geological evidences to magmatic origin of

the deposits. The genesis of porphyry type and hydrothermal vein type deposits are not much controversial, however, the spatio-temporal and genetic relationship between porphyry, skarn and hydrothermal vein type deposits has not been thoroughly studied before.

5.4 Genetic relationships between different types of deposits

In the past few years, we have successively carried out researches of zircon U-Pb geochronology and major-, trace- and rare earth-element geochemistry on mineralization related intrusions in the study area. The results reveal that the Early Cretaceous granitoids of SGXR, including Dongshanwan granitoids, Haobugao granitoids and Huanggang granitoids, show characteristics of A-type granites. And it is broadly accepted that this kind of granites are formed from magmatic underplating in an extensional within plate tectonic environment (Wang, 2015; Li et al., 2015; Wang et al., 2018).

On the basis of analyzed geological and geochemical data, including those published over the past years, we can conclude that the initial ore-bearing hydrothermal fluids of the deposits are mainly derived from magmatic water. The fluid inclusions within minerals from the main-ore stage were cooler and more dilute than those from the pre-ore stage, indicating that the mineralization temperatures and salinities of ore forming fluids tended to decrease with the conduct of the mineralization. And in this process, organic matter from surrounding rocks and meteoric water are also continuously added into the ore-forming fluids, and changed the initial components and isotopic compositions of ore-forming fluids. The formation process of the Early Cretaceous deposits from SGXR can be summarized as follows: during the Early Cretaceous Epoch, intensive underplating of mantle-derived magma led to partial melting of juvenile crust, which further resulting in the emplacement of A-type magma in a post-orogenic extensional tectonic setting. The A-type granites originated from the partial melting of the upper crust with some input of mantle material, resulting in strong differentiation and gradual enrichment in Pb, Zn, Cu, Sn, W, Mo and other ore-forming elements. It appears plausible that the lithospheric thinning not only resulted in emplacement of magmatic rocks and related Sn polymetallic mineralization, but also caused outward migration of mineralizing fluids in a regional thermal gradient. These magmas emplaced at a shallow level and finally formed porphyry-skarn-hydrothermal vein type Sn and associated metal deposits. In some cases, disseminated styles of mineralization with extensive alteration of wall rocks occurred in the top of the intrusions, which finally formed the porphyry deposits with obvious mineralization and alteration zoning characteristics. When the magmatic differentiation hydrothermal fluids migrated to carbonate strata, strong fluid metasomatism occurred at this time, and finally the skarn type deposit formed. Where clastic and/or metamorphic rocks are the country rocks, hydrothermal vein type deposits preferentially formed (Fig. 14). Correspondingly, the spatial distribution of the deposits shows an obvious regularity, that is, from the internal to

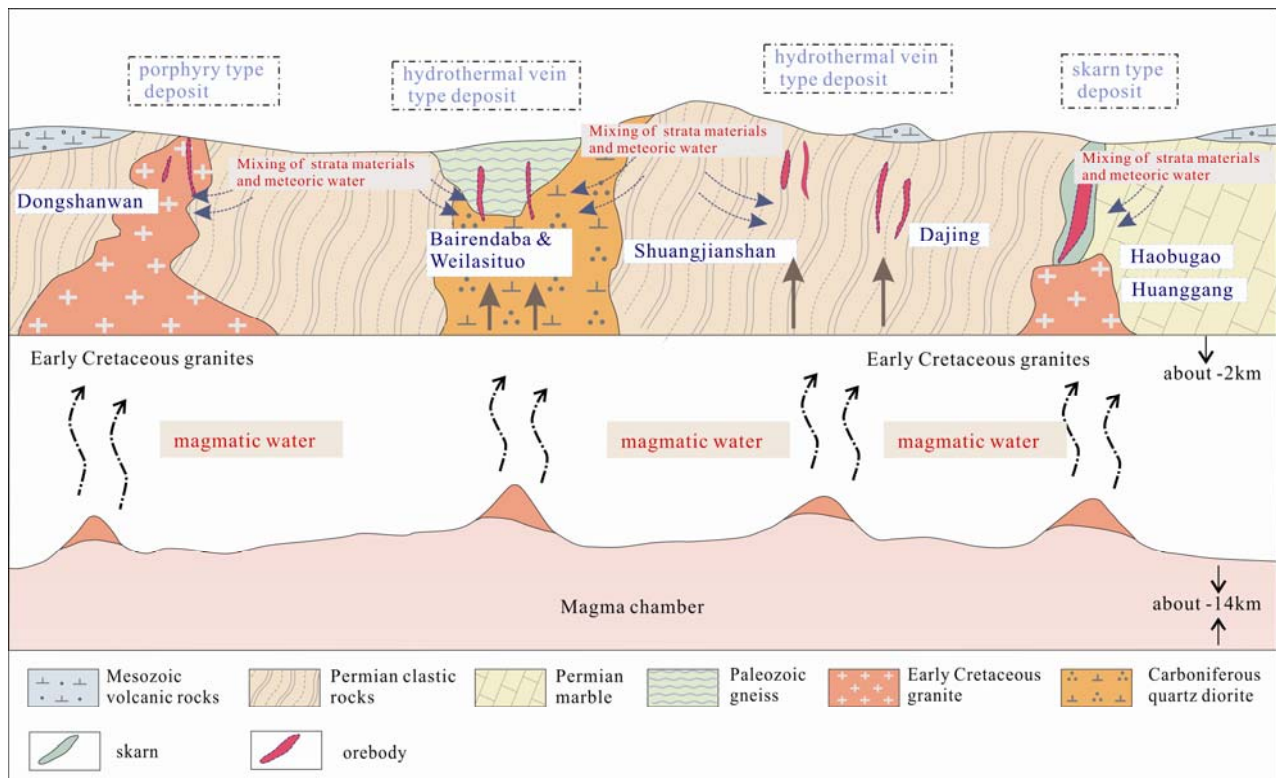


Fig. 14. Metallogenic model and genetic-spatial relationships for skarn, porphyry and hydrothermal vein type deposits in SGXR.

outer zone of the intrusion, porphyry → skarn → vein deposits distribute in order.

6 Conclusions

(1) The Early Cretaceous Sn and associated metal deposits of SGXR can be divided into three principal types according to their geological characteristics: skarn type deposits, porphyry type deposits and hydrothermal vein type deposits.

(2) Fluid inclusion assemblages of different types of deposits are quite different, which represent the complexities of metallogenic process and formation mechanism. And CH_4 and CO_2 have been detected in fluid inclusions of late stage from some of the deposits, indicating that the ore-forming fluids are affected by materials of Permian strata.

(3) Stable isotope data from ore minerals and associated gangue minerals indicate that the initial ore fluids were dominated by magmatic waters, some of which had clearly exchanged oxygen with wall rocks during their passage through the strata. The narrow range for the $\delta^{34}\text{S}$ values presumably reflects the corresponding uniformity of the ore forming fluids, and these $\delta^{34}\text{S}$ values have been interpreted to reflect a magmatic source for the sulfur. The comparison of lead isotope ratios between ores and different geological units also reveal that deeply seated magma has been a significant source of lead in the ores.

(4) Several mineralization related Early Cretaceous granitoids have been identified, and geochemical characteristics of these granites reveal that they were

generated in an intra plate tectonic-magmatic setting. We considered that the porphyry, skarn and vein type deposits formed in the same metallogenic province and developed a metallogenic model for Early Cretaceous Sn and associated metal deposits in the SGXR.

Acknowledgements

The authors thank anonymous reviewers for their constructive comments and suggestions. The paper is supported by Key Discipline Construction Projects of Institute of Disaster Prevention (Quaternary Geology) and Prospecting Projects of National Important Mineral Concentration Areas of Development Research Center of China Geological Survey (0747-1861SITCN149).

Manuscript received May 15, 2019

accepted Aug. 14, 2019

associate EIC XIAO Wenjiao

edited by FEI Hongcai

References

- Ague, J.J., and Brimhall, G.H., 1988. Magmatic arc asymmetry and distribution of anomalous plutonic belts in the batholiths of California: effects of assimilation, crustal thickness, and depth of crystallization. *Geol. Soc. Am. Bull.*, 100(6): 912–927.
- Audétat, A., and Pettke, T., 2006. Evolution of a porphyry-cu mineralized magma system at santarita, New Mexico (USA). *Journal of Petrology*, 47(10): 2021–2046.
- Bao, Q.Z., Zhang, C.J., Wu, Z.L., Wang, H., Li, W., Su, Y.Z., Sang, J.H., and Liu, Y.S., 2006. Carboniferous-Permian marine lithostratigraphy and sequence stratigraphy in Xi Ujimqin Qi, southeastern Inner Mongolia, China. *Geological*

- Bulletin of China, 25(5): 572–579.
- Burnham, C.W., 1980. Late-stage processes of felsic magmatism. *Soc. Mining Geol. Jpn.*, 8: 1–11.
- Chang, Y., and Lai, Y., 2010. Study on characteristics of ore-forming fluid and chronology in the Yindu Ag–Pb–Zn polymetallic ore deposit, Inner Mongolia. *Acta Scientiarum Naturalium Universitatis Pekinensis*, 46(4): 581–593.
- Chu, X.L., and Huo, W.G., 2002. S, C, and Pb isotopes and sources of metallogenic elements of the dajing copper-polymetallic deposit in linxi county, inner mongolia, china. *Acta Petrologica Sinica*, 18(4): 566–574 (in Chinese with English abstract).
- Chu, X., Huo, W., and Zhang, X., 2010. Sulfur, carbon and lead isotope studies of the dajing polymetallic deposit in Linxi county, Inner Mongolia, China – implication for metallogenic elements from hypomagmatic source. *Resource Geology*, 51(4): 333–344.
- Cline, J.S., 1994. Direct evolution of a brine from a crystallizing silicic melt at questa, New Mexico, molybdenum deposit. *Economic Geology*, 89(8): 1780–1802.
- Coleman, M. L., Shepherd, T.J., Durham, J.J., Rouse, J.E., and Moore, G.R., 1982. Reduction of water with zinc for hydrogen isotope analysis. *Analytical Chemistry*, 54(6): 993–995.
- Fan, H.R., Xie, Y.H., Wang, K.Y., and Wilde, S.A., 2004. Methane-rich fluid inclusions in skarn near the giant REE–Nb–Fe deposit at Bayan Obo, northern China. *Ore Geology Reviews*, 25(3): 301–309.
- Feng, J.Z., Ai, X., Wu, Y.B., and Liu, G.B., 1994. Stable isotope geochemistry of Dajing polymetallic deposit. *Geology of Jilin*, 13(3): 60–66 (in Chinese).
- Ge, M.C., Zhou, W.X., Yu, Y., Sun, J.J., Bao, J.Q., and Wang, S.H., 2011. Dissolution and supracrustal rocks dating of Xilin Gol Complex, Inner Mongolia, China. *Earth Sciences Front*, 18(5): 182–195 (in Chinese with English abstract).
- Halter, W.E., Heinrich, C.A., and Pettke, T., 2005. Magma evolution and the formation of porphyry Cu–Au ore fluids: Evidence from silicate and sulfide melt inclusions. *Mineral Deposita*, 39(8): 845–863. doi:10.1007/s00126-004-0457-5
- Harris, A.C., Kamenetsky, V.S., White, N.C., Blevin, P., Jones, M., and Chappel, B., 2003. The magmatic–hydrothermal transition: volatile separation in silicic rocks at Najo de la Alumbrera porphyry Cu–Au deposit, NW Argentina. In *Magmas to mineralization: the Ishihara Symposium*, Geoscience Australia, 14: 69–74.
- Hoefs, J., 1997. *Stable Isotope Geochemistry* (3rd Edition). Springer Verlag, Berlin (1–201).
- Dawei, H., Shiguang, W., Xilin, X., Jisheng, Z., and Tao, W., 2003. Metallogenic province derived from mantle sources: Nd, Sr, S and Pb isotope evidence from the Central Asian orogenic belt. *Gondwana Research*, 6(4): 711–728.
- Jiang, B.B., Zhu, X.Y., Huang, X.K., Xu, Q., Zhang, Z.Q., 2017. Isotopic characteristics of sulfur and lead and metallogenic mechanism of shuangjianzishan silver polymetallic deposit in Inner Mongolia. *Mineral Exploration*, 8(06): 1010–1019. (in Chinese with English abstract)
- Jiang, S.H., Nie, F.J., Liu, Y.F., and Yun, F., 2010. Sulfur and lead isotopic compositions of bairendaba and weilasituo silver-polymetallic deposits, Inner Mongolia. *Mineral Deposits*, 29(1): 101–112 (in Chinese with English abstract)
- Jiang, S.H., Nie, F.J., Bai, D.M., Liu, Y.F., and Yan, L., 2011. Geochronology evidence for indosinian mineralization in Baiyinnuoer Pb–Zn deposit of Inner Mongolia. *Mineral Deposits*, 30(5): 787–798 (in Chinese with English abstract).
- Li, J.W., Shimazaki, H., and Shiga, Y., 2010. Skarns and genesis of the Huanggang Fe–Sn deposit, Inner Mongolia, China. *Resource Geology*, 51(4): 359–376.
- Li, J.F., Wang, K.Y., Lu, J.S., Zhang, X.B., Quan, H.Y., Wang, C.Y., and Wei, L.M., 2015. Ore-forming fluid geochemical characteristics and genesis of Pb–Zn deposit in Hongling, Inner Mongolia. *Earth Science*, 40(6), 995–1005.
- Li, J.F., Wang, K.Y., Quan, H.Y., Sun, F.Y., Zhao, L.S., and Zhang, X.B., 2016. Discussion on the magmatic evolution sequence and metallogenic geodynamical setting background of Hongling Pb–Zn deposit in the southern DaXing'an Mountains. *Acta Petrologica Sinica*, 32(5): 1529–1544 (in Chinese with English abstract)
- Liao, Z., Wang, Y.W., Wang, J.B., Li, H.M., and Long, L.L., 2014. Cassiterite La–mc–icp–ms U–Pb dating of Dajing tin polymetallic deposit in Inner Mongolia and its significance. *Mineral Deposits*, (s1): 421–422 (in Chinese).
- Liu, C., Bagas, L., and Wang, F., 2016. Isotopic analysis of the super-large shuangjianzishanpb–zn–ag deposit in Inner Mongolia, China: constraints on magmatism, metallogenesis, and tectonic setting. *Ore Geology Reviews*, 75: 252–267.
- Liu, J.M., 2004. The regional metallogeny of DaHinggan Ling, China. *Earth Sci. Front*, 11: 269–277.
- Liu, J., Ye, J., Li, Y., Chen, X., and Zhang, R., 2001. A preliminary study on exhalative mineralization in Permian Basins, the southern segment of the Da Hinggan Mountains, China—case studies of the Huanggang and Dajing deposits. *Resource Geology*, 51(4): 345–358.
- Liu, J.M., Zhang, R., and Zhang, Q.Z., 2004. The regional metallogeny of Dahingganling, China. *Earth Science Frontiers* (in Chinese with English abstract).
- Liu, L., Zhou, T., Zhang, D., Yuan, F., Liu, G., Zhao, Z., and White, N., 2018. S isotopic geochemistry, zircon and cassiterite U–Pb geochronology of the Haobugao Sn polymetallic deposit, southern Great Xing'an Range, NE China. *Ore Geology Reviews*, 93: 168–180.
- Liu, W., Li, X.J., and Tan, J., 2003. Fluid mixing as the mechanism of formation of the Dajing Cu–Sn–Ag–Pb–Zn ore deposit, Inner Mongolia—fluid inclusion and stable isotope evidence. *Science in China (Series D)*, 46: 652–662.
- Liu, Y., Nie, F., and Jiang, S., 2014. The Bairendaba and Weilasituo polymetallic sulfide ore system of Inner Mongolia, China: the role of metal fractionation in the genesis of zonation. *Acta Geologica Sinica (English Edition)*, 88(s2): 101–101.
- Liu, Y., Jiang, S. H., Bagas, L., Han, N., Chen, C.L., and Kang, H., 2017. Isotopic (C–O–S) geochemistry and Re–Os geochronology of the Haobugao Zn–Fe deposit in Inner Mongolia, NE China. *Ore Geology Reviews*, 82: 130–147.
- Liu, Y., Jiang, S., and Bagas, L., 2016. The genesis of metal zonation in the Weilasituo and Bairendaba Ag–Zn–Pb–Cu–(Sn–W) deposits in the shallow part of a porphyry Sn–W–Rb system, Inner Mongolia, China. *Ore Geology Reviews*, 75: 150–173.
- Lu, H.Z., Fan, H.R., and Ni, P., 2004. *Fluid inclusions*. Beijing: Science Press (in Chinese).
- Ma, X.H., Chen, B., Lai, Y., Lu, Y.H., 2009. Petrogenesis and mineralization chronology study on the Aolunhua porphyry Mo deposit, Inner Mongolia, and its geological implications. *Acta Petrol. Sin.*, 25: 2939–2950 (in Chinese with English abstract).
- Mei, W., Lü, X., Cao, X., Liu, Z., Zhao, Y., Ai, Z., Tang, R., and Munir, M.A., 2015. Ore genesis and hydrothermal evolution of the Huanggang skarn iron–tin polymetallic deposit, Southern Great Xing'an range: evidence from fluid inclusions and isotope analyses. *Ore Geology Reviews*, 64(1): 239–252.
- Ni, P., Wang, G. G., Yu, W., Chen, H., Jiang, L.L., Wang, B.H., Zhang, H.D., and Xu, Y.F., 2015. Evidence of fluid inclusions for two stages of fluid boiling in the formation of the giant Shapinggou porphyry Mo deposit, Dabieorogen, Central China. *Ore Geology Reviews*, 65: 1078–1094.
- Niu, S.Y., Sun, A.Q., Wang, B.D., Liu, J.M., Guo, L.J., Hu, H. B., and Xu, C.S., 2008. Source of ore-forming materials and mineralization of the Dajing Cu–Sn polymetallic deposit, Inner Mongolia. *Geology in China*, 4, 017.
- Niu, S.Y., Sun, A.Q., Wang, B.D., Nie, F.J., Jiang, S.H., Shao, J.A., Guo, L.J., and Liu, J.M., 2009. Mantle branch structure in the south-central segment of the DaHinggan Mts., Inner Mongolia and its ore-controlling role. *Acta Geologica Sinica (English Edition)*, 83: 1148–1162.
- Ohmoto, H., and Rye, R., 1979. Isotopes of sulfur and carbon. *Geochemistry of hydrothermal ore deposits*, 509–567.
- Ouyang, H., 2013. Metallogenesis and dynamics background of Bairendab–Weilasituo Ag polymetallic deposit in the southern of Great Xing'an Range. *China University of Geosciences (Beijing)*, 19–29 (in Chinese)

- Ouyang, H., Mao, J., Zhou, Z., and Su, H., 2015. Late Mesozoic metallogeny and intracontinental magmatism, southern Great Xing'an Range, northeastern China. *Gondwana Research*, 27 (3): 1153–1172.
- Pan, X.F., Guo, L.J., Wang, S., Xue, H.M., Hou, Z.Q., Tong, Y., and Li, Z.M., 2009. Laser microprobe Ar–Ar dating of biotite from the Weilasituo Cu–Zn polymetallic deposit in Inner Mongolia. *Acta Petrologica Mineralogica*, 28(5): 473–479.
- Quan, H.Y., Cai, W.Y., Zhang, X.B., Fu, L.J., and Wang, K.Y., 2017. Characteristics of fluid inclusions and genesis of weilasituo pb-zn deposit, innermongolia. *Global Geology*, 36 (01): 105–117 (in Chinese with English abstract)
- Roedder, E., 1971. Fluid inclusion studies on the porphyry-type ore deposits at Bingham, Utah, Butte, Montana, and Climax, Colorado. *Economic Geology*, 66: 98–118.
- Roedder, E., and Bodnar, R., 1980. Geologic pressure determinations from fluid inclusion studies. *Annual Review of Earth and Planetary Sciences* 8: 263–301.
- Rowins, S.M., 2000. Reduced porphyry copper-gold deposits: A new variation on an old theme. *Geology*, 28(6), 491–494.
- Shao, J.A., Mou, B.L., Zhu, H.Z., and Zhang, L.Q., 2010. Material source and tectonic setting of the Mesozoic mineralization of the Da Hinggan Mts. *Acta Petrologica Sinica*, 26(3): 649–656 (in Chinese with English abstract).
- Sheng, J.F., and Fu, X.Z., 1999. Metallogenetic environment and geological characteristics of copper-polymetallic ore deposits in middle part of Da Hinggan Mts. *Seismological Publishing House*, 139–169.
- Taylor Jr, H.P., 1979. Oxygen and hydrogen isotope relationships in hydrothermal mineral deposits. *Geochemistry of Hydrothermal Ore Deposits*, 236–277.
- Van den Kerkhof, A., and Thiéry, R., 2001. Carbonic inclusions. *Lithos*, 55(1–4): 49–68.
- Vasyukova, O., Kamenetsky, V. S., and Gömann, K., 2008. Origin of quartz eyes' and fluid inclusions in mineralized porphyries. In 18th Annual VM Goldschmidt Conference, 72: A978.
- Wan, D., Li, J., Wang, Y., Wang, K., Wang, Z., and Wei, L., 2014. Re-os radiometric dating of molybdenite in hongling lead-zinc polymetallic deposit, Inner Mongolia, and its significance. *Earth Science*, 39(6): 687–695.
- Wang, L.J., 2000. Study of tin and copper metallogenetic fluid from Dajing deposit and its genetic significance. *Acta Petrol. Sinica*, 16: 609–614.
- Wang C.Y., Wang K.Y., Liu G.H., Fu L.J., Quan H.Y., 2018a. Characteristics of fluid inclusions and stable isotopes from hydrothermal vein-type deposits in southern Great Xing'an Range, China: implications to genesis of the deposits. *Geological Journal of China Universities*, 24(4): 491–503 (in Chinese with English abstract).
- Wang, C., Li, J., and Wang, K., 2019. Fluid inclusions, stable isotopes, and geochronology of the Haobugao Lead - Zinc deposit, Inner Mongolia, China. *Resource Geology*, 69(1): 65–84.
- Wang, C., Li, J., Wang, K., Yu, Q., and Liu, G., 2018b. Geology, fluid inclusion, and stable isotope study of the skarn-related Pb–Zn (Cu–Fe–Sn) polymetallic deposits in the southern Great Xing'an Range, China: implications for deposit type and metallogenesis. *Arabian Journal of Geosciences*, 11(5): 88.
- Wang, C.Y., 2015. Lead-zinc polymetallic metallogenic series and prospecting direction in Huanggangliang-Ganzhulmiao metallogenic belt, Inner Mongolia (Doctoral dissertation, Jilin University).
- Wang, F., Bagas, L., Jiang, S., and Liu, Y., 2017. Geological, geochemical, and geochronological characteristics of Weilasituo Sn-polymetal deposit, Inner Mongolia, China. *Ore Geology Reviews*, 80: 1206–1229.
- Wang, L.J., Wang, J.B., Wang, Y.W., and Li L.L., 2015. Metallogenic mechanism of fluid and prospecting forecast of dajing Sn-Cu polymetallic deposit, Inner Mongolia. *Acta Petrologica Sinica*, 31(4): 991–1001 (in Chinese with English abstract).
- Wang, J., Hou, Q. Y., Chen, Y. L., Liu, J. B., Wang, Z., and Leng, F. R., 2010. Fluid inclusion study of the Weilasituo Cu polymetal deposit in Inner Mongolia. *Geoscience*, 24(5): 847–855.
- Wang, L.J., Shimazaki, H., and Shiga, Y., 2001. Skarns and genesis of the Huanggang Fe - Sn deposit, Inner Mongolia, China. *Resource Geology*, 51(4): 359–376.
- Wang, X., Xu, D., Lv, X., Wei, W., Mei, W., Fan, X., and Sun, B., 2018. Origin of the Haobugao skarn Fe-Zn polymetallic deposit, Southern Great Xing'an Range, NE China: Geochronological, geochemical, and Sr-Nd-Pb isotopic constraints. *Ore Geology Reviews*, 94(1): 58–72.
- Wang, X.D., 2017. Diagenesis and mineralization of Ag-Pb-Zn polymetallic deposits in Lindong area, Inner Mongolia. China University of Geosciences. (in Chinese).
- Wang, Y.W., Wang, J.B., Uemoto, T., and Wang, L.J., 2010. Geology and mineralization at the Dajing tin - polymetallic ore deposit, Inner Mongolia, China. *Resource Geology*, 51(4): 307–320.
- Wu, F.Y., Sun, D.Y., Ge, W.C., Zhang, Y.B., Grant, M.L., Wilde, S.A., and Jahn, B.M., 2011. Geochronology of the Phanerozoic granitoids in northeastern China. *Journal of Asian Earth Sciences*, 41(1): 1–30.
- Wu, G., Chen, Y.J., Sun, F.Y., Li, J.C., Li, Z.T., and Wang, X.J., 2008. Geochemistry of the late Jurassic granitoids in the northern end area of Da Hinggan Mountains and their geological and prospecting implications. *Acta Petrologica Sinica*, 24: 899–910 (in Chinese with English abstract).
- Xiao, W., Windley, B.F., Allen, M.B., and Han, C., 2013. Paleozoic multiple accretionary and collisional tectonics of the Chinese Tianshan orogenic collage. *Gondwana Research*, 23(4): 1316–1341.
- Xu, J.H., Xie, Y.L., Ding, R.F., Yin, Y.J., Shan, L.H., and Zhang, G.R., 2007. CO₂-CH₄ fluids and gold mineralization: southern margin of Altay, China and Muruntau of Uzbekistan. *Acta Petrologica Sinica*, 3(8): 2026–2032.
- Ye, J., Liu J.M., Zhang, A.L., Zhang, R.B., 2002. Petrological evidence for exhalative mineralization: case studies of Huanggang and Dajing deposits in the southern segment of the Da Hinggan Mountains, China. *Acta Petrologica Sinica* 18(4): 588–592 (in Chinese with English abstract).
- Ying, J.F., Zhou, X.H., Zhang, L.C., and Wang, F., 2010. Geochronological framework of Mesozoic volcanic rocks in the Great Xing'an Range, NE China, and their geodynamic implications. *Journal of Asian Earth Sciences*, 39(6): 0–793.
- Zeng, Q.D., Liu, J.M., Jia, C.S., Wan, Z.M., Chang-Ming, Y.U., and Jie, Y.E., 2007. Sedimentary exhalative origin of the Baiyinnuoer Zinc-Lead deposit, Chifeng, Inner Mongolia: geological and sulfur isotope evidence. *Journal of Jilin University*, 37(4): 659–667 (in Chinese with English abstract).
- Zeng, Q., Liu, J., Yu, C., Jie, Y., and Liu, H., 2011. Metal deposits in the Da Hinggan Mountains, NE China: Styles, characteristics, and exploration potential. *International Geology Review*, 53(7): 846–878.
- Zeng, Q., Liu, J., Zhang, Z., Jia, C., Yu, C., Ye, J., and Liu, H., 2009. Geology and lead isotope study of the Baiyinnuoer Zn-Pb-Ag deposit, south segment of the Da Hinggan Mountains, northeastern China. *Resource Geology*, 59(2): 170–180.
- Zhai, D., Liu, J., Zhang, H., Yao, M., Wang, J., and Yang, Y., 2014. S–Pb isotopic geochemistry, U–Pb and Re–Os geochronology of the Huanggangliang Fe–Sn deposit, Inner Mongolia, NE China. *Ore Geology Reviews*, 59(6): 109–122.
- Zhai, D.G., Liu, J.J., and Li, J.M., 2016. Geochronological study of Weilasituo porphyry type Sn deposit in Inner Mongolia and its significance. *Mineral Deposits*, 35(5): 1011–1022 (in Chinese with English abstract).
- Zhang, X.B., Wang, K.Y., Wang, C.Y., Li, W., Yu, Q., Wang, Y.C., and Huang, G.H., 2017. Age, genesis, and tectonic setting of the Mo-W mineralized Dongshanwan granite porphyry from the Xilamulun metallogenic belt, NE China. *Journal of Earth Science*, 28(3): 433–446.
- Zhao, Y.M., and Zhang, D.Q., 1997. Metallogeny and prospective evaluation of copper-polymetallic deposits in the Da Hinggan Mountains and its adjacent regions. *Press, Beijing*, 48–82 (in Chinese with English abstract).
- Zhou, Z.H., Linsu, L., and Feng, J.R., 2010a. Molybdenite re-ages of Huanggang skarn Sn-Fe deposit and their geological significance, Inner Mongolia. *Acta Petrologica Sinica*, 26(3):

- 667–679.
- Zhou, Z.H., Wang, A.S., and Tao, L.I., 2011. Fluid inclusion characteristics and metallogenic mechanism of huanggangsn-fe deposit in Inner Mongolia. *Mineral Deposits*, 30(5): 867–889.
- Zhou, Z., Lü, L., Yang, Y., and Li, T., 2010b. Petrogenesis of the Early Cretaceous a-type granite in the Huanggang Sn-Fe deposit, Inner Mongolia: constraints from zircon u-pb dating and geochemistry. *Acta Petrologica Sinica*, 26(12): 3521–3537.
- Zhou, Z.H., Mao, J.W., and Lyckberg, P., 2012. Geochronology and isotopic geochemistry of the A-type granites from the HuanggangSn-Fe deposit, southern Great Hinggan Range, NE China: implication for their origin and tectonic setting. *Journal*

of Asian Earth Sciences, 49: 272–286.

About the first and corresponding author



WANG Chengyang, male; born in 1988 in Qufu City, Shandong Province; doctor; graduated from Jilin University; lecturer of Institute of Disaster Prevention. He is now interested in the study on mineral resource prospecting and exploration in Southern of Great Xing'an Range. Email: 598648597@qq.com; Phone: 13932675615.